



ARTICLE

Two distinct colonic CD14⁺ subsets characterized by single-cell RNA profiling in Crohn's disease

Laurence Chapuy¹, Marwa Bsati¹, Siranush Sarkizova^{2,3}, Manuel Rubio¹, Amélie Therrien^{1,4}, Evelyne Wassef¹, Mickael Bouin⁴, Katarzyna Orlicka⁴, Audrey Weber⁴, Nir Hacohen³, Alexandra-Chloé Villani^{3,5} and Marika Sarfati¹

Inflammatory bowel diseases are associated with dysregulated immune responses in the intestinal tissue. Four molecularly identified macrophage subsets control immune homeostasis in healthy gut. However, the specific roles and transcriptomic profiles of the phenotypically heterogeneous CD14⁺ macrophage-like population in inflamed gut remain to be investigated in Crohn's disease (CD). Here we identified two phenotypically, morphologically and functionally distinct colonic HLADR⁺SIRPα⁺CD14⁺ subpopulations that were further characterized using single-cell RNA-sequencing (scRNAseq) in CD. Frequencies of CD64^{hi}CD163^{-dim} cells selectively augmented in inflamed colon and correlated with endoscopic score of disease severity. IL-1β and IL-23-producing CD64^{hi}CD163^{-dim} cells predominated over TNF-α-producing CD64^{hi}CD163^{hi} cells in lesions. Purified "inflammatory monocyte-like" CD163⁻, but not "macrophage-like" CD163^{hi} cells, through IL-1β, promoted Th17/Th1 but not Th1 responses in tissue memory CD4⁺T cells. Unsupervised scRNAseq analysis that captures the entire HLADR⁺SIRPα⁺ population revealed six clusters, two of which were enriched in either CD163⁻ or CD163^{hi} cells, and best defined by *TREM1/FCAR/FCN1/IL1RN* or *CD209/MERTK/MRC1/CD163L1* genes, respectively. Selected newly identified discriminating markers were used beyond CD163 to isolate cells that shared pro-Th17/Th1 function with CD163⁻ cells. In conclusion, a molecularly distinct pro-inflammatory CD14⁺ subpopulation accumulates in inflamed colon, drives intestinal inflammatory T-cell responses, and thus, might contribute to CD disease severity.

Mucosal Immunology (2019) 12:703–719; <https://doi.org/10.1038/s41385-018-0126-0>

INTRODUCTION

The interplay between genetic, environmental, and immunological factors contributes to the pathogenesis of Crohn's disease (CD), a chronic inflammatory bowel disease (IBD) that results from an inappropriate immunologic response to the commensal microflora.^{1,2} Several experimental models of colitis were developed in syngeneic mice to unravel CD pathogenesis.³ However, none of them entirely recapitulates the complex clinical and histopathological features that are observed in CD patients, emphasizing the need to examine the immune response in human gut disease tissues.⁴ Intestinal immune infiltrate is composed of T helper (Th) cell subsets,⁵ granulocytes,^{6,7} mononuclear phagocyte (MNP) populations⁸, as well as rare innate lymphoid cells (ILCs).^{9,10} Mucosal MNPs, which includes macrophages (Mφ), monocyte-derived cells and dendritic cells (DCs), expressing or not CD14 and SIRPα,^{11–13} contribute to gut homeostasis. Therefore, investigating the function and molecular profile of the MNP population, which is phenotypically heterogeneous in inflamed gut mucosa, has clear implication in better understanding IBD pathophysiology.¹⁴

A large population of human intestinal resident Mφ actively maintains healthy steady-state conditions. Previous studies reported that these Mφ lack CD14 and CD64 expression, are anergic in response to Toll-like receptor (TLR) stimulation, and retain phagocytic functions.¹⁵ However, it was recently proposed

that recruitment and maturation of human monocytes into four Mφ subsets expressing various levels of CD14 and retaining endocytic function occurred in jejunum at homeostasis.¹³ A similar maturation process was previously demonstrated in murine gut lamina propria where Mφ arise from Ly6C^{hi} monocytes, which are continuously recruited to the mucosa. These cells differentiate towards TLR-hyporesponsive Mφ that secrete IL-10 and express CD64 at steady state.¹⁶

In addition to intestinal resident Mφ, conventional DC (cDCs) subsets that drive the polarization of naive CD4 T cells^{12,17} are key players in the maintenance of regulatory T-cell-mediated intestinal homeostatic conditions.¹⁸ Briefly, two cDC subsets stratified by SIRPα and CD103 expression levels in humans and mice have been reported in gut homeostatic state.^{12,19–21} More specifically, human SIRPα⁻cDC1s that express CD103 represent a minor population in the gut,^{20,22} which is related to circulating CLEC9A⁺CD141⁺cDC1.¹² The CD103⁺SIRPα⁺cDC2 are the predominant cDC population in the ileum²² and are related to circulating CD1c⁺cDC2.²³ In contrast, CD103⁻SIRPα⁺cDC2s predominate in the colon but are the less characterized cDC population.^{24,25} In fact, these CD103⁻SIRPα⁺ cells, which reportedly clustered with blood monocytes, might include monocyte-derived cells.¹² Noteworthy, markers commonly associated with circulating monocytes and cDC2 appeared to be more broadly expressed than previously

¹Immunoregulation Laboratory, Centre de Recherche du Centre Hospitalier de l'Université de Montréal (CRCHUM), Université de Montréal, Montréal, QC, Canada; ²Department of Biomedical Informatics, Harvard Medical School, Boston, MA, USA; ³Broad Institute of MIT and Harvard, Cambridge, MA, USA; ⁴Centre Hospitalier de l'Université de Montréal (CHUM), Université de Montréal, Montréal, QC, Canada and ⁵Center for Immunology and Inflammatory Diseases, Massachusetts General Hospital, Boston, MA, USA
Correspondence: Marika Sarfati (m.sarfati@umontreal.ca)

Received: 3 October 2018 Revised: 5 December 2018 Accepted: 11 December 2018
Published online: 22 January 2019



appreciated. For example, CD14⁺ monocytes were shown to co-express CD1c,²⁶ a cDC2 marker, while CD1c⁺ DC subsets were reported to express several monocyte markers, including CD14.²⁷

The characterization of the MNP population is far more challenging in human inflamed gut tissue, owing to the heterogeneity of IBD patients with differences in genetic background, disease onset, duration, severity, treatment, and geographic location.²⁸ In mice, it was shown that the maturation process of Ly6C^{hi} monocytes is interrupted during intestinal inflammation favoring the accumulation of an intermediate Ly6C⁺CD64⁺CX₃CR1^{int} monocyte-like cell subset that shows a pro-inflammatory profile.¹⁶ Noteworthy, infusion of autologous circulating radiolabeled CD14⁺ monocytes into CD patients can be retraced as CD14⁺ Mφ-like cells in their inflamed gut mucosa.²⁹ However, analyses deciphering the composition of human CD14⁺ MNP subpopulations in inflamed intestine remain sparse. Kamada et al. reported the presence of a unique CD14⁺ Mφ-like cell population, which produce large amounts of IL-23, IL-1β, IL-6, TNF-α, and IL-10 in the inflamed ileal or colonic mucosa of IBD patients.³⁰ Our previous report showed that HLADR⁺SIRPα⁺ cells, which predominantly include CD14⁺ cells, but also comprise cDC2, selectively accumulate in inflamed colon of CD patients, and that IL-1β and TNF-α secretion was restricted to HLADR⁺SIRPα⁺ cells.¹¹ Yet, the potential heterogeneity of mucosal CD14⁺ MNPs under chronic inflammatory conditions is highlighted by the dual function of these cells. The CX₃CR1⁺CD14⁺ MNPs favor IL-22 production by ILC3 in an IL-23-dependent manner in human mild-inflamed CD mucosa,³¹ suggesting their protective function. Furthermore, several groups of investigators have stratified CD14⁺ MNPs according to their phenotype. CD14⁺HLADR^{high}CD163^{low} Mφ are detected in equal proportions in non-inflamed and inflamed CD or UC mucosa^{32,33}, while CD14⁺HLADR^{dim} are increased in inflamed ileum and colon of CD or UC patients.^{16,34,35} Whether CD14⁺HLADR^{high/dim} MNPs represent molecularly distinct subpopulations endowed with functional diversity in inflamed CD tissues remain unanswered.

The efficacy of Vedolizumab, a monoclonal antibody (mAb) that targets the gut homing integrin α4β7, argues for a T-cell-dependent mechanism in CD patients.³⁶ Studies have provided evidence that HLADR⁺CD14⁺MNPs induce human allogeneic circulating naive T-cell polarization into Th17 or Th17/Th1.^{32,37} Whether and how these cells drive intestinal inflammatory T-cell responses and more particularly promote Th17/Th1 responses in mucosal effector memory CD4⁺ T cells, has not been investigated in inflamed gut mucosa. Double IFN-γ/IL-17-secreting cells are considered pathogenic in mice with colitis³⁸ and in patients with CD.^{5,39,40} The IFN-γ⁺IL-17⁺ cells might arise from Th17 cells, which display a high degree of plasticity.⁴¹ Indeed, Th17 cells, which exert a protective role in the intestine,^{42,43} can acquire a pathogenic signature and function depending on the tissue cytokine environment.⁴² In humans, intestinal Th17 clones can be skewed to produce IFN-γ, shifting to IFN-γ⁺IL-17⁺ (Th17/Th1) and IFN-γ⁺IL-17⁻ (non-classic Th1 or Th1*) cells in the presence of IL-12³⁹ or IL-23.⁴⁴

Here, we assessed the morphology, function and molecular diversity of HLADR⁺SIRPα⁺ MNPs that were stratified by CD14, CD64, and CD163 protein expression, in colonic tissues from a large cohort of CD patients. The CD14⁺CD64^{hi}CD163^{-/dim} and more precisely the CD163⁺ cells selectively accumulated in inflamed CD colon, expressed low levels of TNF-α, and promoted colonic memory Th17 and Th17/Th1 but not Th1 responses in an IL-1β-dependent manner. CD163⁻ cell accumulation in inflamed mucosa was independent of age, gender, disease location, disease behavior, and remarkably, their frequency correlated with endoscopic disease severity. Isolation of CD14⁺ subpopulations from two extremes of CD163 expression spectrum, i.e., CD163⁻ (P3) and CD163^{hi} (P4), led to the identification of two morphologically and molecularly distinct CD14⁺ subsets, while further identifying new discriminating markers that allowed validation of the presence of two distinct functional CD14⁺ subsets.

RESULTS

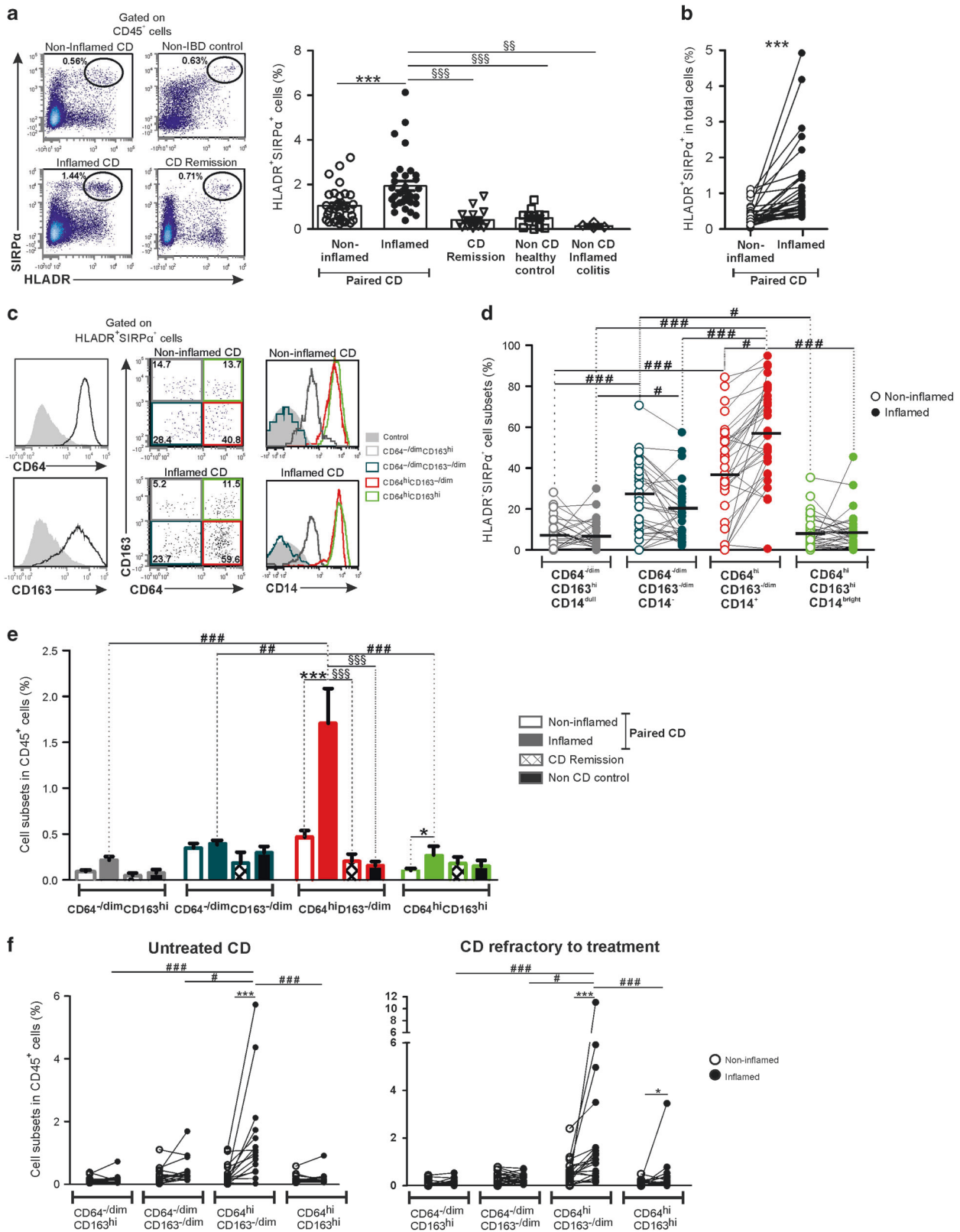
HLADR⁺SIRPα⁺ MNPs comprise two CD14⁺CD64^{hi} subpopulations: accumulation of CD64^{hi}CD163^{-/dim}, but not CD64^{hi}CD163^{hi} cells, in inflamed colon of CD patients

After excluding dead cells, doublets and neutrophils and gating on hematopoietic CD45⁺ cells (Figure S1), the average frequency of HLADR⁺SIRPα⁺ MNPs was significantly greater in inflamed tissues relative to paired non-lesional sites in the colon of patients with CD ($n = 36$) ($P < 0.0001$; Fig. 1a). Considering the increased cellular infiltrate in inflamed CD tissues (mean 54.1% (\pm SD 21.1) versus 34.6% (\pm SD 16.0) CD45⁺ cells in inflamed versus non-inflamed colon), the augmentation of HLADR⁺SIRPα⁺ MNPs in total cells further reflected their accumulation in lesions ($P < 0.0001$; Fig. 1b). We therefore postulated that HLADR⁺SIRPα⁺ MNPs could be associated with disease pathogenesis. The frequency of this population was significantly reduced in healthy colonic mucosa of CD patients in endoscopic remission ($P < 0.0001$; Fig. 1a) to similar levels as those observed in non-inflamed mucosa of CD as well as in healthy non-CD donors ($P < 0.0001$). Moreover, HLADR⁺SIRPα⁺ cells were detected at a lower frequency in inflamed colon of patients with infectious or drug-induced colitis ($P < 0.002$; Fig. 1a) relative to inflamed CD colon.

To assess potential heterogeneity within the HLADR⁺SIRPα⁺ MNPs infiltrating inflamed colon, this population was subdivided according to CD64 and CD163 expression levels (Fig. 1c). CD163, a scavenger receptor expressed on human gut Mφ and CD64 (the Fc-gamma receptor 1), has been reported to be an inflammatory DC or Mφ marker in chronic inflammatory disorders in humans.^{45,46} Four subpopulations were identified: two CD64^{-/dim} (left quadrants) as well as two CD64^{hi} cells (right quadrants) expressing variable intensity of CD163 (i.e., CD163^{-/dim} and CD163^{hi}) (Fig. 1c). Further immunophenotyping highlighted that the two CD64^{hi} populations expressed high levels of CD14 (Fig. 1c); mean fluorescence intensity of SIRPα, its isoform SIRPβ, CX3CR1, or CD103 (Figure S2A) could not discriminate these two CD14⁺ subpopulations. In contrast, HLADR expression was significantly higher in CD64^{hi}CD163^{hi} when compared to CD64^{hi}CD163^{-/dim} cells but reduced in inflamed versus non-inflamed colon in all three subsets examined (Figure S2B). Furthermore, CD64^{-/dim}CD163^{-/dim} cells were CD14⁻ and overrepresented among the HLADR⁺SIRPα⁺ MNPs that expressed CD1c (Figure S2C).

Next, we assessed whether any of the 4 HLADR⁺SIRPα⁺ MNPs subpopulations accumulated in inflamed CD colonic lesions. As depicted in Fig. 1d, only the frequency of one CD14⁺ subset, i.e., the CD64^{hi}CD163^{-/dim} cells, significantly increased in inflamed versus paired non-inflamed mucosa of CD patients ($P < 0.05$). When accounting for the increased percentage of the entire HLADR⁺SIRPα⁺ MNP population in inflamed infiltrate versus non-inflamed colon (Fig. 1a), the accumulation of CD64^{hi}CD163^{-/dim} cells was further highlighted compared to CD in remission and non-CD control donors as well as to paired non-inflamed CD tissue ($P < 0.0001$) (Fig. 1e). The cohort of active CD patients was next subdivided based on treatment history at the time of sample collection (Fig. 1f). The frequencies of CD64^{hi}CD163^{-/dim} cells increased in inflamed when compared to paired non-inflamed colon and remained the predominant HLADR⁺SIRPα⁺ cell subset in both treated and untreated groups. Notably, a slight accumulation of CD64^{hi}CD163^{high} cells was noticed in inflamed relative to non-inflamed samples in patients undergoing treatment.

Overall, these data provide evidence that HLADR⁺SIRPα⁺ MNPs accumulate in inflamed colon of patients with CD. These MNPs are heterogeneous and comprise two CD14⁺CD64^{hi} (CD163^{-/dim} and CD163^{hi}), one CD14⁺ (CD64^{-/dim}CD163^{hi}), and one CD14⁻ (CD64^{-/dim}CD163^{-/dim}) subpopulations. However, only the CD64^{hi}CD163^{-/dim} cells augment in inflamed CD colon.



Frequency of CD64^{hi}CD163^{-dim} cells correlates with disease severity in CD patients and is not modified by treatment history. To assess the potential biological relevance of CD64^{hi}CD163^{-dim} cell accumulation in inflamed CD colon, we measured disease severity using the validated Simple Endoscopic Score for CD (i.e., SES-CD) (Table S1)⁴⁷ in an independent cohort of CD patients. The

data showed that the percentage of CD64^{hi}CD163^{-dim} but not CD64^{hi}CD163^{hi} cells in HLADR⁺SIRPα⁺ MNP⁺ positively correlated with SES-CD ($P < 0.0001$; Fig. 2a). Furthermore, frequencies of CD64^{hi}CD163^{-dim} and CD64^{hi}CD163^{hi} cells were not modified by treatment history that included biologics combined or not with immunosuppressive drugs, in none of the two independent

Fig. 1 Frequencies of CD14⁺CD64^{hi}CD163^{-dim} cells increase in inflamed colon of CD patients. **a** Percentage of colonic HLADR⁺SIRPα⁺ cells after gating on CD45⁺ LPMC in active CD patients (*n* = 36) (paired non-inflamed and inflamed samples, Wilcoxon signed rank test); CD in remission (*n* = 15) and non-CD (healthy, *n* = 12; colitis, *n* = 4) patients (Mann–Whitney test). **b** Percentage of HLADR⁺SIRPα⁺ cells in total cells in active CD patients (*n* = 36, Wilcoxon signed rank test). **c** HLADR⁺SIRPα⁺ MNPs stained for CD64 and CD163 expression, representative histograms with isotype control mAbs (left panels). HLADR⁺SIRPα⁺ MNPs subdivided according to intensity of CD64 and CD163 expression into 4 MNP subpopulations; representative dot plots (middle panels) and CD14 expression (right panels). **d** Frequencies of the 4 MNPs (CD64^{-dim}CD163^{hi}, CD64^{-dim}CD163^{-dim}, CD64^{hi}CD163^{-dim}, CD64^{hi}CD163^{hi} cells) in HLADR⁺SIRPα⁺ cells in paired non-inflamed and inflamed CD patients (*n* = 36, Friedman test). **e** Percentage of the 4 MNPs in CD45⁺ cells in paired non-inflamed and inflamed CD patients (*n* = 36), CD in remission (*n* = 15), and non-CD control (*n* = 12) patients (Wilcoxon signed rank, Mann–Whitney and Friedman tests). **f** Frequencies of the 4 MNPs in CD45⁺ LPMC in paired non-inflamed and inflamed tissues in untreated CD patients (*n* = 15, left panel) and those refractory to treatment (*n* = 21, right panel) (Wilcoxon signed rank and Friedman tests). For (a, e, f), *P* < 0.01 threshold for significance in Wilcoxon signed rank test and Mann–Whitney test to account for test multiplicity

cohorts examined separately (Fig. 2b). We therefore combined the two cohorts (*n* = 97) and showed that age, gender, age at diagnosis, disease location (L2 and L3) and disease behavior (B1, B3, and B3) did not influence the percentage of HLADR⁺SIRPα⁺ MNPs or CD64^{hi}CD163^{-dim} and CD64^{hi}CD163^{hi} cells in HLADR⁺SIRPα⁺ MNPs (Figure S3A, B, C, D and E). Remarkably, the CD64^{hi}CD163^{-dim} cells remained the predominant HLADR⁺SIRPα⁺ cell subset in CD colon, regardless the parameters used for stratification of CD patients, with the exception of colonic tissue from CD patients with penetrating B3 disease, in which the average frequency of CD64^{hi}CD163^{-dim} was slightly reduced.

Collectively, these observations indicate that one particular CD14⁺ subpopulation, the CD64^{hi}CD163^{-dim} cells, accumulates in inflamed CD colon in proportions that correlate with disease severity regardless of treatment history, demographics, and disease classification.

CD64^{hi}CD163^{-dim} cells are the major contributors to IL-23 and IL-1β secretion but not TNF-α in inflamed CD colon Building on the previous report of TNF-α and IL-1β production being restricted to SIRPα⁺ cells in inflamed CD colon,¹¹ we examined which of CD14⁺CD64^{hi} cell subset expressed pro-inflammatory cytokines *ex vivo* (Fig. 3). Frequencies of TNF-α-producing-cells were higher in CD64^{hi}CD163^{hi} cells between non-inflamed and inflamed colonic tissues (*P* < 0.05), undetectable or low in CD64^{hi}CD163^{-dim} and CD64^{-dim}CD163^{-dim} cells, and observed in only 2/15 patients in the CD64^{-dim}CD163^{hi} cells (Fig. 3a and Figure S4A). In contrast, the percentages of IL-23-producing-cells were significantly more abundant in CD64^{hi}CD163^{-dim} and CD64^{hi}CD163^{hi} cells in inflamed mucosal samples (*P* < 0.001 in 13/15 patients and *P* < 0.05 in 9/15 patients, respectively) while their frequencies were lower in the two CD64^{-dim} subpopulations. Despite the fact that both CD14⁺CD64^{hi} subpopulations produced IL-1β, only IL-1β-producing CD64^{hi}CD163^{-dim} cells were significantly enriched in inflamed versus non-inflamed mucosal samples (CD64^{hi}CD163^{-dim}, *P* < 0.02; CD64^{hi}CD163^{hi}, *P* = 0.4), and detected at variable but low frequencies in CD64^{dim} cells. IL-6 levels were highly variable in CD14⁺CD64^{hi} subsets across the different tissue states tested, and higher in CD64^{hi} compared to CD64^{-dim} cells. Furthermore, when considering the increased frequencies of HLADR⁺SIRPα⁺ MNPs in inflamed colon, TNF-α-producing CD64^{hi}CD163^{hi} cells were more frequent than TNF-α-producing CD64^{hi}CD163^{-dim} cells (*P* < 0.004). Conversely, IL-23⁻ (*P* < 0.0005) and IL-1β⁻ (*P* < 0.03) producing CD64^{hi}CD163^{-dim} cells were higher than CD64^{hi}CD163^{hi} cells in CD45⁺ cells (Fig. 3b). Treatment including biologics did not influence the frequencies of cytokine-producing-cells in either of the CD14⁺CD64^{hi} subsets (Figure S4B). We further examined the expression of anti-inflammatory cytokine IL-10 in the two CD14⁺CD64^{hi} subsets (Figure S4C). The percentage of IL-10-producing-cells, as well as IL-10 expression per cell were higher in CD64^{hi}CD163^{hi} relative to CD64^{hi}CD163^{-dim} cells in inflamed colon (*P* < 0.002). Finally, single IL-23 or IL-1β-producing-cells predominated in CD64^{hi}CD163^{-dim} when compared to CD64^{hi}CD163^{hi} cells in 3/4 patients examined (Fig. 3c and Figure S4D).

Overall, these results highlight that among the 4 HLADR⁺SIRPα⁺ MNP subsets, the CD64^{hi}CD163^{-dim} cells accumulate in greater proportions in inflamed CD mucosa and are thus the major contributor to IL-23 and IL-1β. CD64^{hi}CD163^{hi} cells represent the major TNF-α or IL-10-producing-cells in inflamed colon.

Colonic CD64^{hi}CD163⁻ (P3) cells skew autologous CD4⁺ T cells towards Th17/Th1 responses in CD patients

We next asked whether and how the colonic CD14⁺ subsets influenced the Th17/Th1 profile of autologous CD4⁺ T cells in CD patients. To this end, we simultaneously purified from inflamed CD colon, CD4⁺ T cells that were depleted of CD25⁺ regulatory T cells, as well as CD14⁺CD64^{hi} subpopulations at the two extremes of CD163 expression spectrum (i.e., CD163⁻ and CD163^{hi}), thus excluding the CD163^{dim} cells (Fig. 4a). Noteworthy, within the CD163^{-dim} subpopulation, the CD163⁻ cells remained the predominant subpopulation that significantly infiltrated the inflamed colon while the frequency of CD163^{dim} cells did not increase relative to paired non-inflamed sites (Figure S5A). Furthermore, the frequency of CD163⁻, but not CD163^{dim} cells correlated with the endoscopic disease severity (*P* < 0.0002, *r* = 0.46, Spearman test). The two highly purified CD14⁺CD64^{hi} subsets were hereafter named P3 (CD163⁻) and P4 (CD163^{hi}) cells with P3 cells displaying a kidney shaped nucleus and a reduced cell size when compared to P4 cells, that exhibited typical Mφ morphology with vacuoles (Figure S5B). The intermediate CD14^{-dim}CD64^{dim} (P1) and the triple negative CD14⁻CD64⁻CD163⁻ cells (P2) were morphologically heterogeneous populations and therefore not further examined in functional studies.

Data in Fig. 4b indicated that in the context of co-culture with P3 cells was a significantly greater proportion of IFN-γ⁺IL-17⁺ and IFN-γ⁻IL-17⁺ cells in colonic CD4⁺ T cells observed (*P* < 0.002), with no effect on IFN-γ⁺IL-17⁻ T cells. The low yield of P4 cells, which represented on average less than 0.2% of HLADR⁺SIRPα⁺ MNPs in CD45⁺ cells (Fig. 1e), precluded performing more than three co-cultures experiments. However, the P4-Mφ-like cells did not appear to augment memory intestinal Th17, Th17/Th1, or Th1 responses.

Noteworthy, colonic CD4⁺ T cells contained higher frequencies of cells displaying phenotypes associated with Th1 (CCR6⁻CXCR3⁺) and Th17/Th1 (CCR6⁺CXCR3⁺) in inflamed mucosa when compared to their mesenteric lymph node (MLN) counterparts (Fig. 4c). In contrast, Th17 (CCR6⁺CXCR3⁻) cells represented more than 25% of CD4⁺ T cells in inflamed MLNs and less than 10% in inflamed CD colon (*P* < 0.001; Fig. 4c). In this context, we further asked whether CCR6⁺CXCR3⁻CD62L^{low}CD4⁺ (Th17 T_{EM}) MLN cells that recently migrated to the colon could be readily shaped by P3 cells to acquire a Th17/Th1 cytokine profile. To this end, Th17 T_{EM} were purified from either MLN or colon and co-cultured with colonic P3 cells. Th17/Th1, Th17 but not Th1, responses were significantly augmented by P3 cells in CCR6⁺CXCR3⁻ T_{EM} cells (Fig. 4d). Note that the minor colonic CCR6⁺CXCR3⁻ T_{EM} subset comprised increased frequencies of single IFN-γ-producing-cells (~50%), relative to their MLN (~2%) counterpart. Finally, P3 cells increased the frequency of IL-6⁺TNF-α⁻ (*P* < 0.03) and IL-6⁺TNF-α⁺ (*P* < 0.03) cells in CCR6⁺CXCR3⁻ T_{EM} cells (Figure S6).

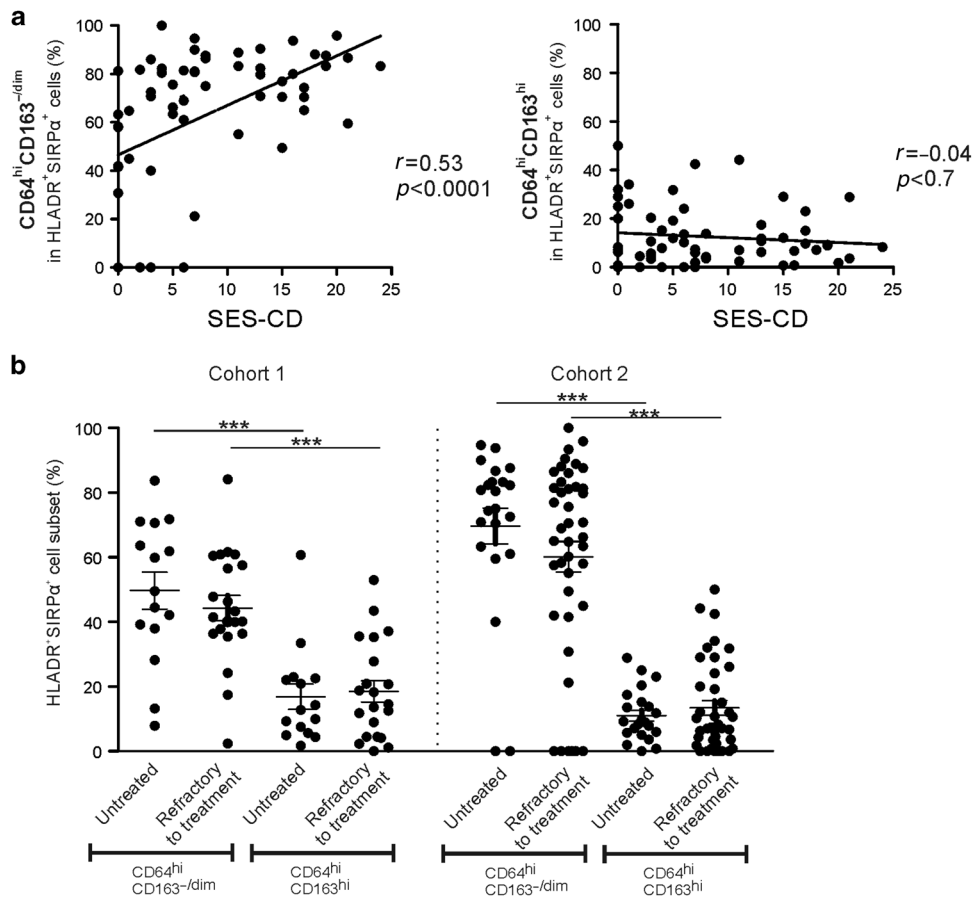


Fig. 2 Frequencies of CD14⁺CD64^{hi}CD163^{-dim} cells correlate with disease severity. **a** Correlation between the percentage of CD64^{hi}CD163^{-dim} (left panel) and CD64^{hi}CD163^{high} cells (right panel) and the endoscopic score of disease severity (inflamed colon of active CD patients, SES-CD > 3, *n* = 46; healed colon of CD in remission SES-CD ≤ 2, *n* = 15) (Spearman's rank correlation test). **b** Frequencies of CD64^{hi}CD163^{-dim} and CD64^{hi}CD163^{hi} cells in the two treated or untreated independent cohorts examined (cohort 1, *n* = 36 and cohort 2, *n* = 61). Wilcoxon signed rank test and Mann-Whitney test were used. *P* < 0.01 threshold for significance to account for test multiplicity

Collectively, P3 cells shift Th17 towards a Th17/Th1 profile while contribute to further augment the local Th17 response.

CD64^{hi}CD163⁻ (P3) cells promote colonic Th17 and Th17/Th1 responses in an IL-1β-dependent manner in CD patients. We next investigated some of the mechanisms by which P3 cells, along with the IL-1β and IL-23 they secrete, can govern mucosal Th17 and Th17/Th1 profile. Neutralizing IL-1β function in P3/CD4⁺ T-cell co-cultures inhibited Th17 and Th17/Th1 responses elicited by P3 cells (*P* < 0.03) (Fig. 5a). Accordingly, addition of recombinant IL-1β to purified colonic CD4⁺ T cells significantly increased the frequency of IFN-γ⁺IL-17⁺ (*P* < 0.002), IFN-γ⁺IL-17⁻ (*P* < 0.002) but not IFN-γ⁻IL-17⁻ cells (Fig. 5b), along with enhancing IL-17, IFN-γ, GM-CSF, TNF-α, and IL-6 secretion in the culture supernatant (Fig. 5c). The presence of IL-23 augmented the percentage of IFN-γ⁻IL-17⁺ (*P* < 0.04) and IFN-γ⁺IL-17⁺ (*P* < 0.03) in mucosal CD4⁺ T cells. In contrast, IL-12 addition decreased IFN-γ⁻IL-17⁺ (*P* < 0.007) while increasing IFN-γ⁺IL-17⁻ cells (*P* < 0.04) (Fig. 5d) along with IFN-γ, GM-CSF, and IL-6 production (Fig. 5e). Noteworthy, the opposite IL-17 expression in colonic CD4⁺ T cells stimulated by either recombinant IL-23 or IL-12 (Fig. 5d, e), which both share the IL-12p40 chain, reflects the lack of significant inhibition of Th17 responses when adding neutralizing anti-IL-12p40 mAb to CD4⁺ T/P3 cells co-cultures (Fig. 5f).

Taken collectively, IL-1β secreted by the P3 cells, as well as IL-23, contribute towards amplifying a potential pathogenic Th17 signature in CD mucosa.

Unsupervised single-cell RNA-sequencing (scRNAseq) independently segregates clusters enriched in P3 or P4 cells. To further assess whether P3 and P4 cells indeed represent molecularly distinct subpopulations, we performed unsupervised scRNAseq analyses according to the gating strategy depicted in Fig. 6a. Since this experimental approach aimed to comprehensively sample all the MNPs defined by the HLADR⁺SIRPa⁺ gate, single cells isolated from inflamed colonic mucosa of three CD patients were thus sorted from five overlapping gates consisting of P3, CD64^{hi}CD163^{dim} (Px), P4 as well as P1 and P2, which collectively capture the full spectrum of HLADR⁺SIRPa⁺ MNPs, and then profiled using a modified version of Smart-Seq2 protocol.²⁷ Unbiased clustering analyses of all HLADR⁺SIRPa⁺ single cells revealed six general clusters (Fig. 6b). The single-cell identity making up each cluster was reported in Table S2. Clusters E and F consisted of a majority of P3 and P4 cells, respectively, a significant enrichment over a random assortment of cells into clusters (*P* < 0.01 for both comparisons; chi-square test) (Fig. 6b). Thus, the remaining cells comprised in clusters E and F originated from sorting gates Px and P1 that were designed to capture likely transitioning population (Fig. 6a). More precisely, cluster E comprised 50% P3, 32% Px and 11% P1 while cluster F comprised 50% P4, 17% Px and 13% P1. These two clusters were enriched in CD14-expressing cells with cluster F expressing higher CD14 levels than cluster E (Figure S7A and Table S3), corroborating the data observed at the protein level in the two CD64^{hi} subsets (*P* < 0.05; Figure S7B). Collectively, these observations support the concept that CD163 effectively stratified two CD14⁺CD64^{hi} subpopulations.

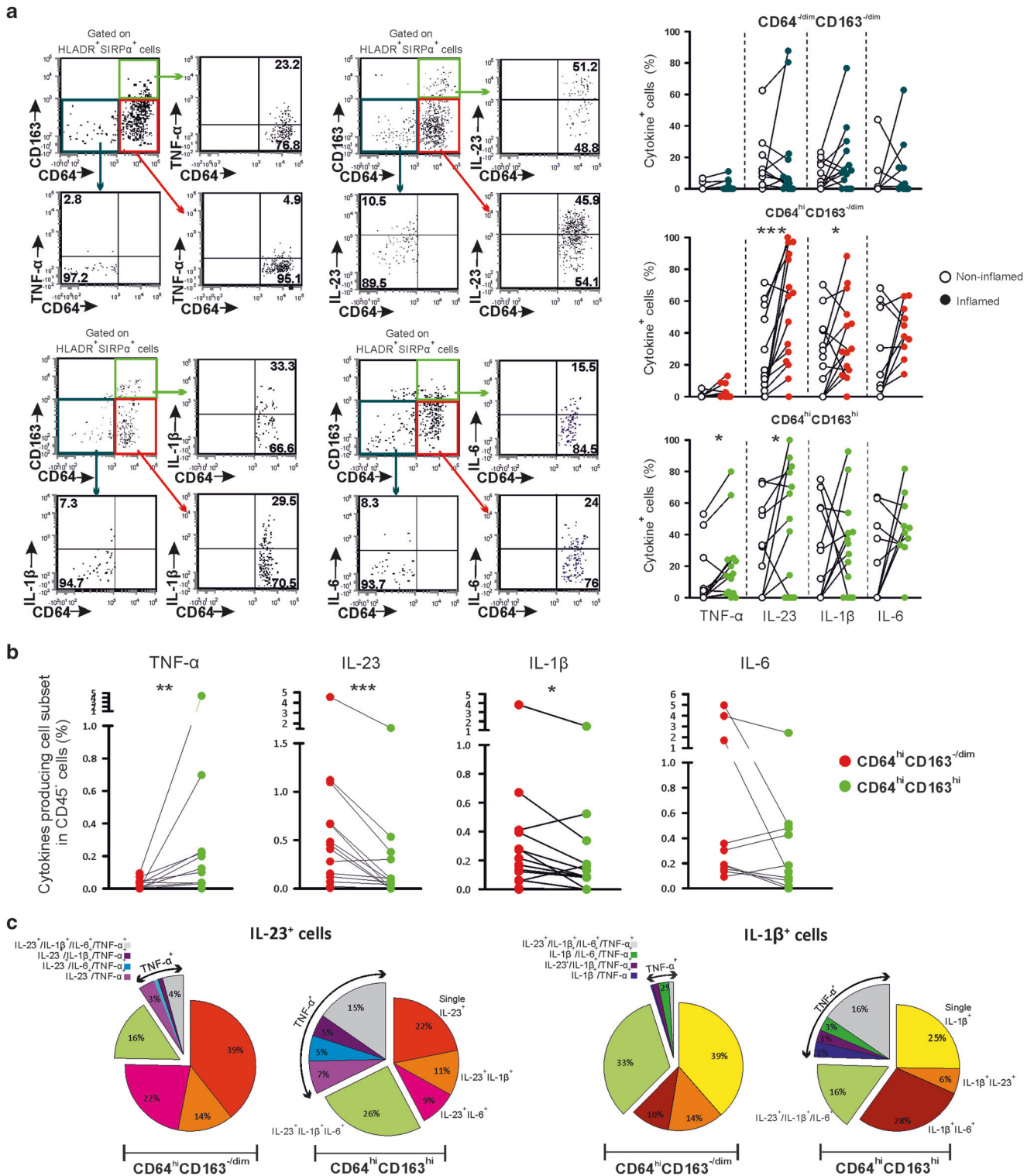


Fig. 3 CD64^{hi}CD163^{-/dim} cells are the major contributors to IL-23 and IL-1 β secretion but not TNF- α in inflamed CD colon. **a** Frequencies of TNF- α ($n=13$), IL-23 ($n=15$), IL-1 β ($n=14$), and IL-6 ($n=11$)-producing-cells among CD64^{-/dim}CD163^{-/dim}, CD64^{hi}CD163^{-/dim}, and CD64^{hi}CD163^{hi} cells in paired non-inflamed and inflamed CD colon. Dot plots are one representative experiment in inflamed colon. **b** Frequencies of cytokine-producing CD64^{hi}CD163^{-/dim} and CD64^{hi}CD163^{hi} subsets in CD45⁺ cells in inflamed colon: TNF- α ($n=13$), IL-23 ($n=15$), IL-1 β ($n=14$), and IL-6 ($n=11$). **c** Co-expression of IL-1 β , IL-6, IL-23p19, and TNF- α in the two CD14⁺CD64^{hi} subsets in inflamed CD mucosa ($n=4$): proportion of single, double, triple, and quadruple producing-cells among IL-23⁺ (left panels) and IL-1 β ⁺ cells (right panels). **a, b** Wilcoxon signed rank test

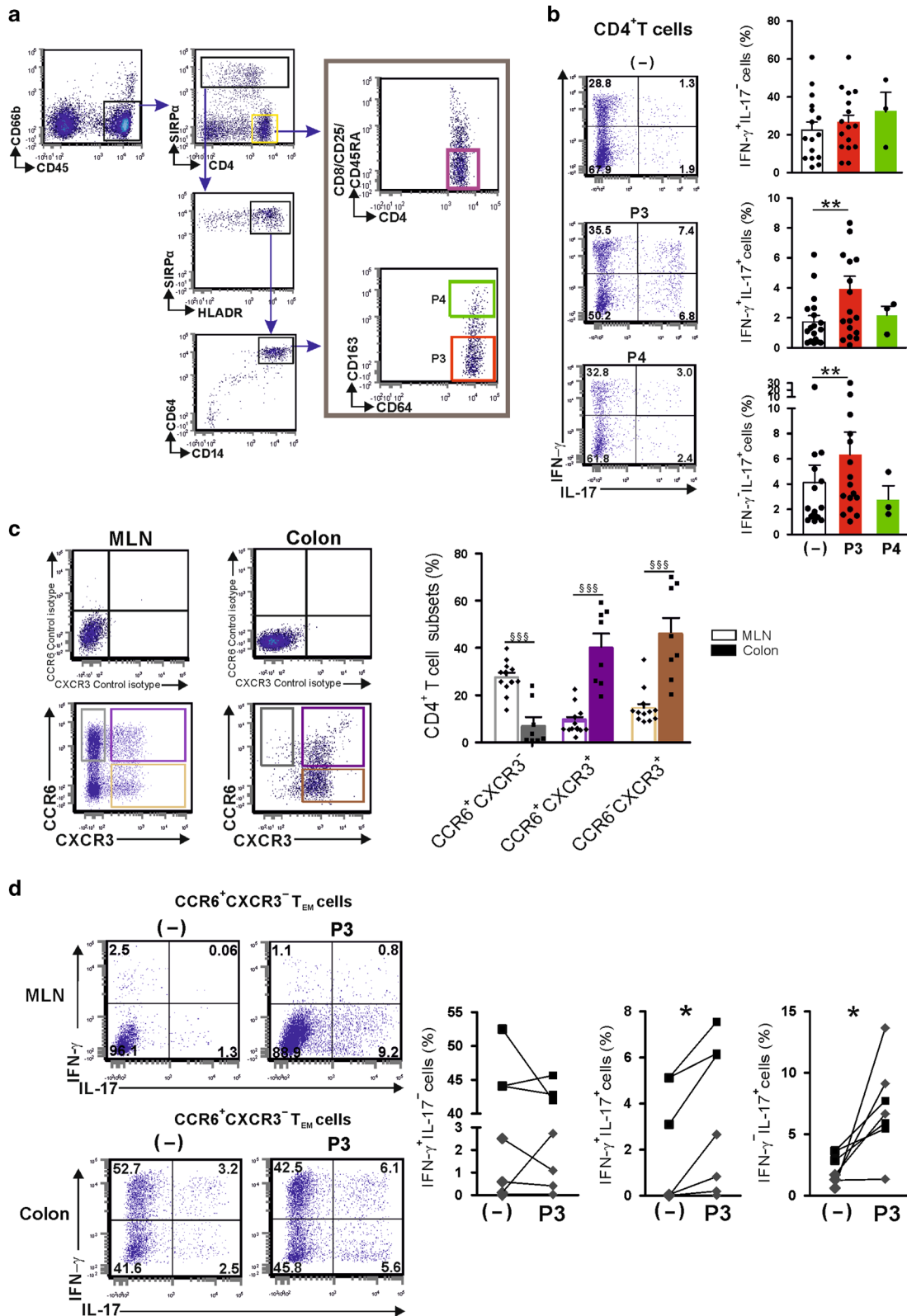


Fig. 4 CD64^{hi}CD163⁻ (P3) cells shape autologous CD4⁺ T cells towards a Th17/Th1 profile. **a** Gating strategy for sorting CD4⁺ T cells (purple gate), P3 (red gate) and P4 (green gate) cells in inflamed CD colon. **b** P3 and P4 cells were co-cultured with autologous colonic CD4⁺ T cells for 6 days. IL-17/IFN- γ expression was measured using intracytoplasmic staining after gating on CD3⁺ T cells (P3, $n = 16$; P4, $n = 3$) (Wilcoxon signed rank test). **c** Distribution of CCR6⁺CXCR3⁻ (Th17), CCR6⁺CXCR3⁺ (Th17/Th1), CCR6⁻CXCR3⁺ (Th1) cells in MLN ($n = 8$) and colon ($n = 12$) of CD patients (Mann-Whitney test). **d** CCR6⁺CXCR3⁻ CD62^{low}CD4⁺ cells isolated from MLN (diamond, $n = 4$) or inflamed CD colon (square, $n = 3$) were co-cultured with autologous P3 cells for 6 days. IL-17 and IFN- γ expression assessed using intracytoplasmic staining after gating on CD3⁺ T cells (Wilcoxon signed rank test)

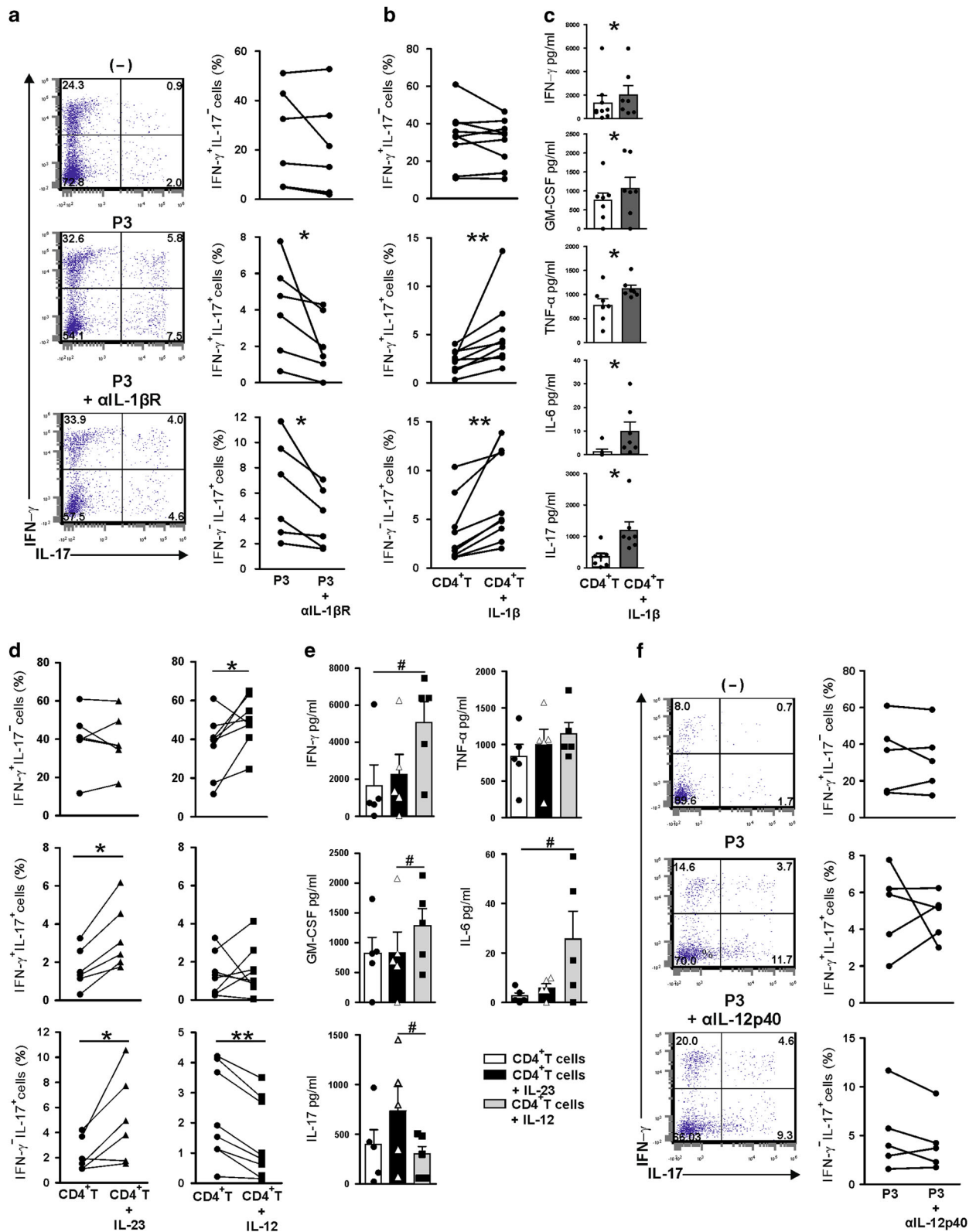


Fig. 5 CD64^{hi}CD163⁻ (P3) cells augment colonic Th17 and Th17/Th1 responses in an IL-1 β -dependent manner. CD4⁺ T cells, P3 and P4 cells were purified from inflamed CD colons as in Fig. 4A. CD4⁺ T cells were stimulated with anti-CD3 and anti-CD28 beads and: **a** co-cultured with P3 cells in the presence or absence of α IL-1 β R; **b**, **c** cultured with or without IL-23 or IL-12; **d**, **e** cultured with or without IL-23 or IL-12; **f** co-cultured with P3 cells in the presence or absence of α IL-12p40. **a** ($n = 6$), **b** ($n = 10$), **d** ($n = 7$), and **f** ($n = 5$): intracytoplasmic IL-17/IFN- γ expression after gating on CD3⁺ T cells. **c** ($n = 7$) and **e** ($n = 5$): multiplex dosage in the culture supernatant. **a-d**, **f** Wilcoxon signed rank test; **e** Friedman test

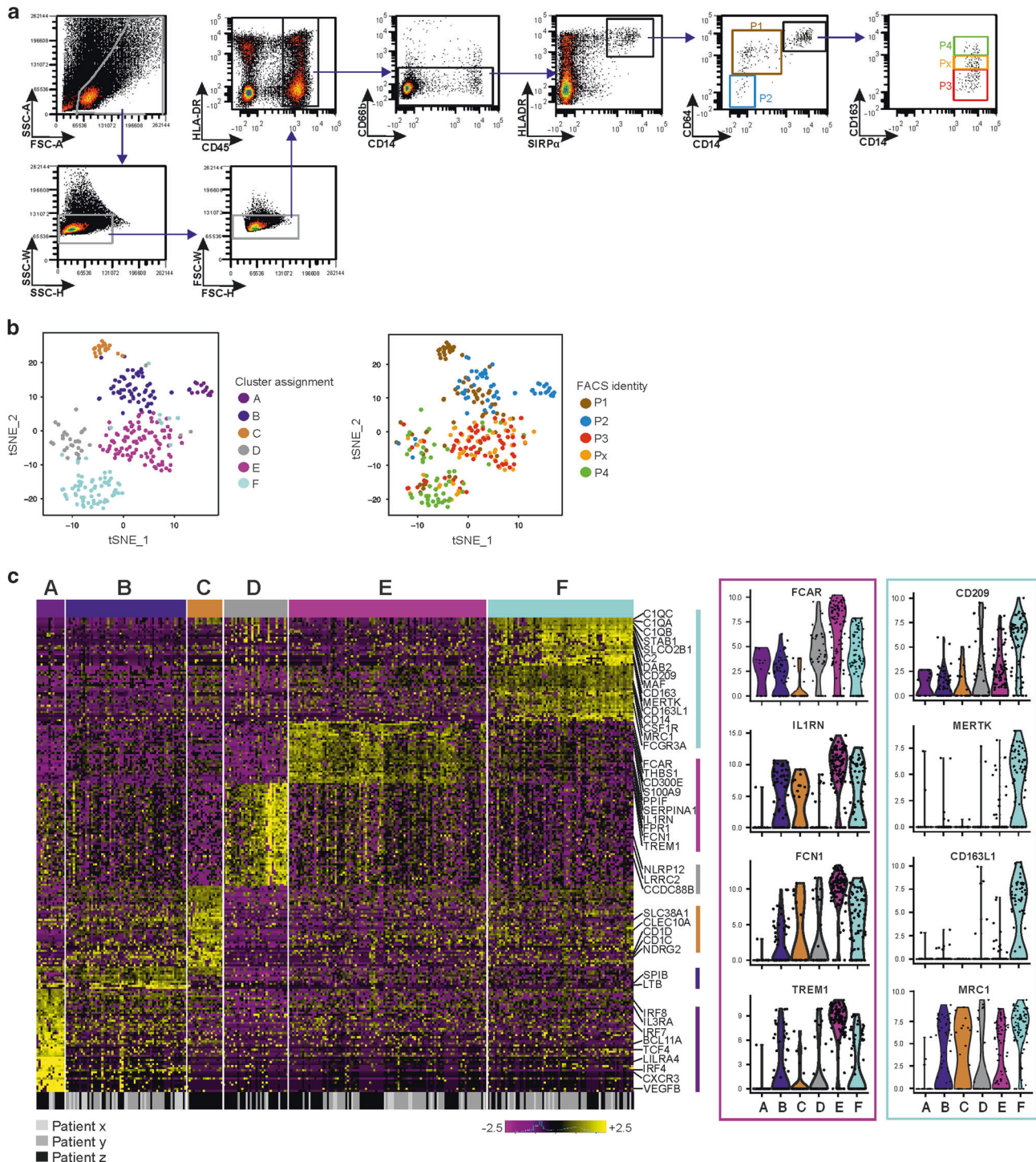


Fig. 6 scRNAseq analysis of HLADR⁺SIRP α ⁺ MNP population for scRNAseq analysis. **a** Gating strategy to capture the entire HLADR⁺SIRP α ⁺ cell population for scRNAseq analysis. Single cells were sorted across overlapping gates labeled as P1 (brown), P2 (blue), P3 (red), Px (orange), and P4 (green) from 3 patients. **b** t-SNE visualization of isolated single HLADR⁺SIRP α ⁺ cells from all five gates ($n = 294$ cells that passed QCs), colored by cluster assignment (left) and FACS identity (right). **c** Heatmap reports scaled expression (log TPM + 1 (Transcripts Per Million) values) of discriminative gene set (AUC cutoff ≥ 0.75 ; average log fold change expression difference ≥ 1.2) for each cluster defined. Heatmap color scheme is based on z-score distribution from -2.5 (purple) to 2.5 (yellow). Color legend at the top of the heatmap indicates the unbiased cluster assignment as defined in panel (b) and color legend at the bottom of the heatmap indicates the CD patient identity ($n = 3$; labeled "x", "y", and "z"). Violin plots illustrate gene expression level distribution of discriminating surface marker genes (y-axis, $\log_2(\text{TPM} + 1)$) across each of the six identified clusters (x-axis)

As shown in Fig. 6c and Table S3, cluster A encompassed a subpopulation of the P2 gate bearing pDC markers (e.g., *BCL11A*, *TCF4*, *LILRA4*, *VEGFB*), while genes in cluster B (e.g., *SPIB*, *LTB*) and C (e.g., *CD1C*, *SLC38A1*) characterized conventional DCs, and

contained most of the remaining P2 along with P1 cells (Fig. 7). While cluster D also expressed myeloid cell markers (*NLRP12*, *LRRC2*, *CCDC88B*), these cells were best defined by their general downregulation of several genes associated with the ubiquitin-

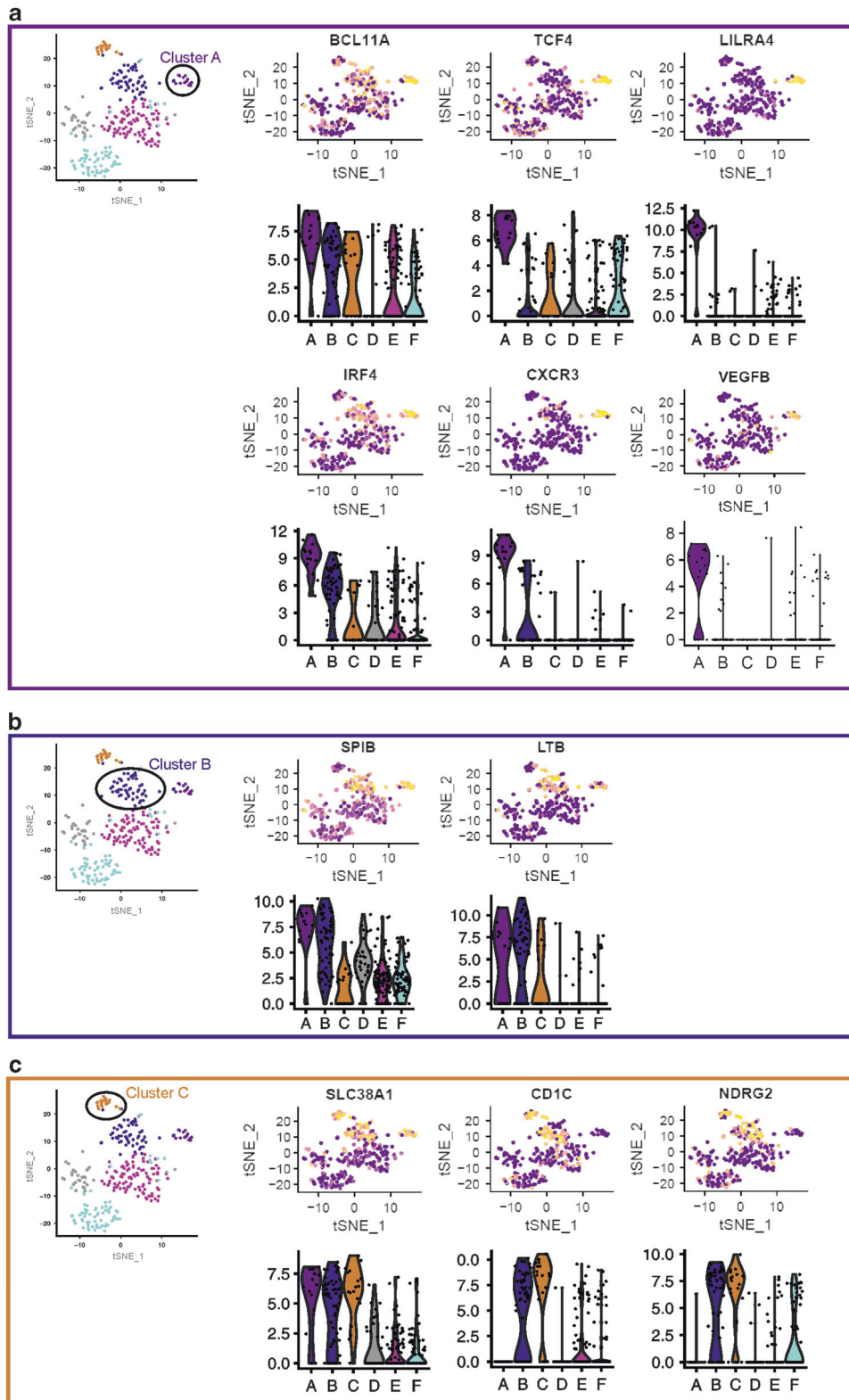


Fig. 7 Gene expression of discriminating genes of cluster (**a**, **b**, **c**). Feature plots of key discriminating genes expressed in particular single-cell cluster, consisting of the t-SNE plot from Figure 6b on which is overlaid the gene expression level of selected markers for cluster (**a**, **b**, **c**). Color scheme is according to $\log_2(\text{TPM} + 1)$ expression value, with color gradient from purple (low) to yellow (high) expression. Violin plots illustrate expression level distribution of discriminating surface marker genes (y-axis, $\log_2(\text{TPM} + 1)$) across each of the six identified clusters (x-axis). Genes overexpressed in **a** cluster A, **b** cluster B, and **c** cluster C are depicted

proteasome system (UPS) (e.g., *PSMA6*, *PSMB1*, *UBE2L6*) (Figure S7C). Clustering analysis was consistent across the three CD patients profiled and allowed the identification of additional discriminating markers beyond CD163 that could be used to isolate cells for the functional analyses. Examples of markers for cluster E (enriched for P3 cells) included *TREM1*, *FCAR*, *FCN1*, *IL1RN*, and *FPR1*, while those for cluster F (enriched for P4 cells) included *CD163L1*, *MERTK*, *CD209*, *MRC1* and a set of complement genes (e.g., *C2*, *C1QA*, *C1QB*, *C1QC*) (Fig. 8).

Together, single cell RNA-sequencing analyses empowered a finer cellular classification of the HLADR⁺SIRPα⁺ MNP, showing

the existence of six clusters in CD inflamed colon and potentially identified new discriminative markers for P3 and P4 cells.

TREM⁺CD209⁻MERTK⁻(P3/b) cells promote colonic Th17 and Th17/Th1 responses in CD patients

Our subsequent analyses focused on the newly identified surface markers that were differentially expressed in cells included in clusters E and F. Single cells expressing *TREM1* and *FCAR* predominated in cluster E, while *MRC1*, *MERTK*, and *CD209*-expressing cells were observed in cluster F (Fig. 9a). In fact, *TREM1* and *CD89* (*FCAR*), as well as *CD206* (*MRC1*), *CD209*, and *MERTK*

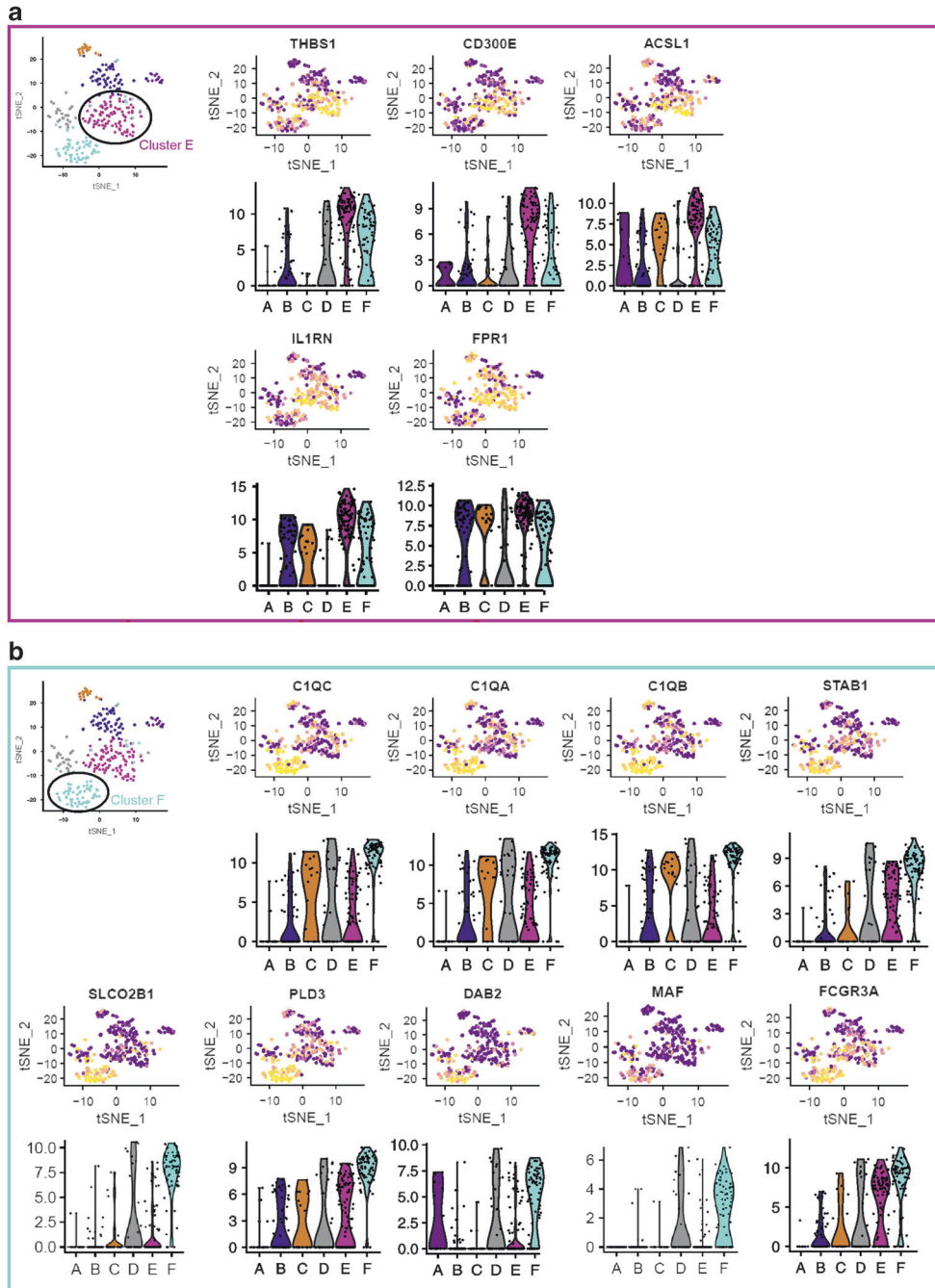


Fig. 8 Gene expression of selected discriminating genes of cluster E and F. Feature plots of key discriminating genes expressed in particular single-cell cluster, consisting of the t-SNE plot from Figure 6b on which is overlaid the gene expression level of selected markers for cluster E and F. Color scheme is according to log₂(TPM + 1) expression value, with color gradient from purple (low) to yellow (high) expression. Violin plots illustrate expression level distribution of discriminating surface marker genes (y-axis, log₂(TPM + 1)) across each of the six identified clusters (x-axis). Genes overexpressed in (a) cluster E and (b) cluster F are depicted in feature plots and associated violin plots

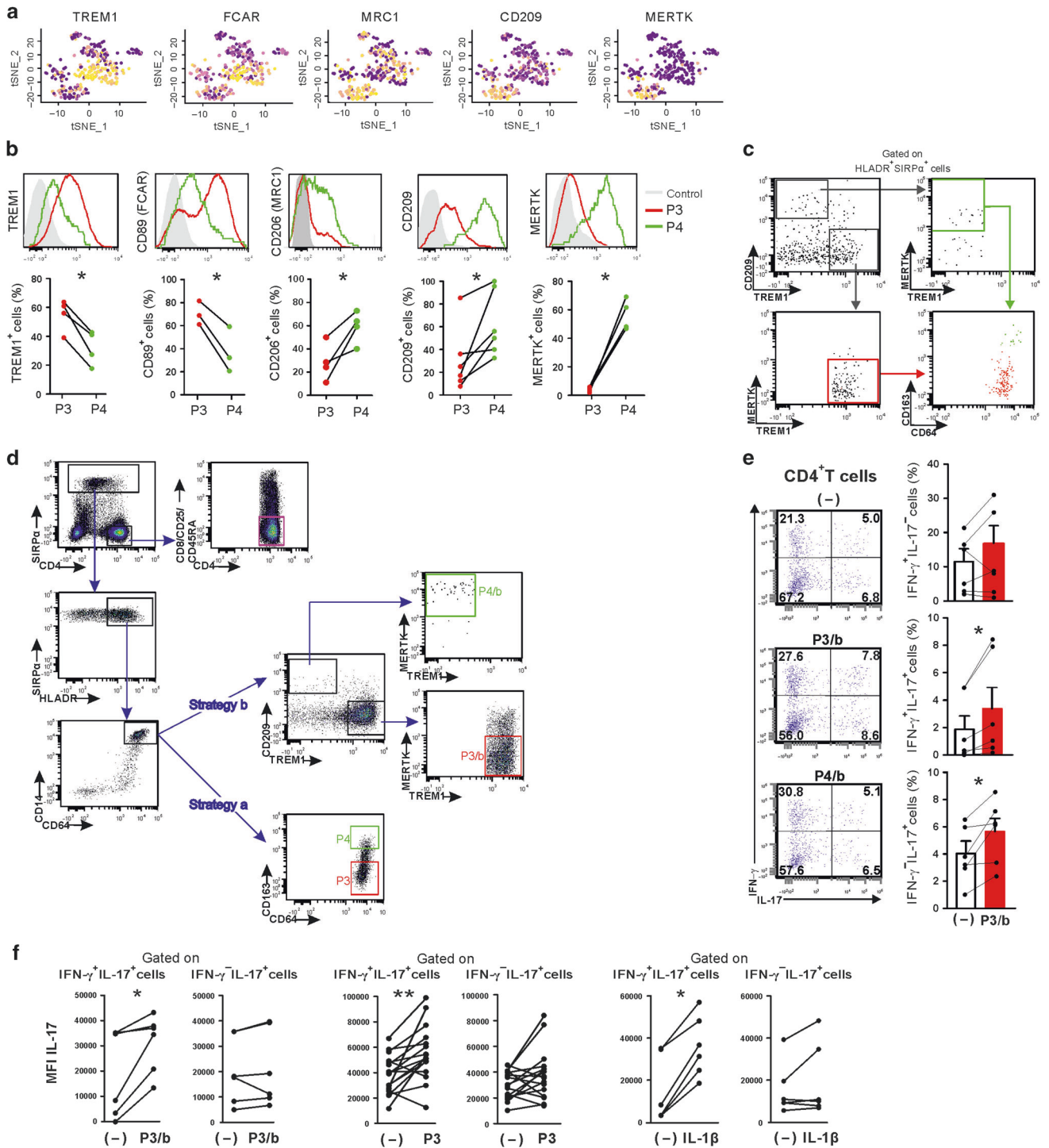


Fig. 9 Functional validation of P3 and P4 cells using the newly identified phenotype by scRNAseq. **a** Feature plots of key discriminating genes consisting of the t-SNE plot from Figure 6B on which is overlaid the gene expression level of selected markers genes (TREM1, FCAR, MRC1, CD209, and MERTK) for cluster E and F. Color scheme is according to $\log_2(\text{TPM} + 1)$ expression value, with color gradient from purple (low) to yellow (high) expression. **b** TREM1 ($n = 4$) and CD89 ($n = 3$), CD206 ($n = 4$), CD209 ($n = 6$), and MERTK ($n = 4$) protein expression in the two CD14⁺CD64^{hi}CD163⁻ subsets after gating on HLADR⁺SIRP α ⁺ cells. **c** TREM1⁺CD209⁻MERTK⁻ cells display P3 (CD64^{hi}CD163⁻) phenotype and TREM1⁻CD209⁺MERTK⁺ cells show P4 (CD64^{hi}CD163^{hi}) markers. Shown is one representative experiment among four. **d** Gating strategy for isolation of CD4⁺ T cells and MNPs: strategy b (TREM1⁺CD209⁻MERTK⁻, P3/b and TREM1⁻CD209⁺MERTK⁺, P4/b) in comparison to strategy a, as depicted in Fig. 4. **e** Representative dot plots of CD4⁺ T cells co-cultured with autologous colonic P3/b ($n = 6$) and P4/b ($n = 2$) cells for 6 days (left panels); IL-17/IFN- γ expression measured via intracytoplasmic staining after gating on CD3⁺ T cells (right panels). **f** Mean fluorescence intensity of IL-17 in colonic CD4⁺ T cells co-cultured for 6 days with autologous P3/b ($n = 6$), P3 ($n = 16$) or in the presence of IL-1 β ($n = 6$). **b, e, f**, Wilcoxon signed test

protein expression was validated as P3 and P4 cells markers, respectively (Fig. 9b), with TREM1⁺CD209⁻MERTK⁻ (P3/b) cells expressing P3 (CD64^{hi}CD163⁻) phenotype and TREM1⁻CD209⁺MERTK⁺ (P4/b) cells expressing P4 (CD64^{hi}CD163^{hi}) phenotype (Fig. 9c). Colonic P3/b and P4/b cells were next purified following the gating strategy b when compared to strategy a used to isolate P3 cells (Fig. 9d). P3/b, but not P4/b cells, augmented Th17 and Th17/Th1 but not Th1 responses ($P < 0.03$ and $P < 0.04$, respectively) in autologous CD4⁺ T cells (Fig. 9e), corroborating the function of P3 cells (Fig. 4). The low frequency of P4/b, like P4, cells, limited the study of their function to only two out of six experiments. Interestingly, P3/b and P3 cells along with IL-1 β significantly upregulated the mean fluorescence intensity of IL-17 (IL-17 MFI) ($P < 0.03$, $P < 0.004$, $P < 0.03$, respectively) in colonic IFN- γ ⁺IL-17⁺ but not IFN- γ ⁻IL-17⁺ CD4⁺ T cells, highlighting an increase in IL-17 expression in Th17/Th1 cells only (Fig. 9f). Collectively, scRNAseq analyses identified new discriminative markers, confirming the existence of one HLADR⁺SIRP α ⁺ subpopulation, namely the inflammatory monocyte-like CD14⁺CD64^{hi}CD163⁻TREM1⁺CD209⁻MERTK⁻ cells that promoted Th17 and Th17/Th1 responses in inflamed colon of CD patients.

DISCUSSION

Several attempts to characterize the phenotype and function of HLADR⁺CD14⁺ MNPs infiltrating inflamed CD mucosa highlight their potential heterogeneity.^{11,30–32,34,35,48} In the present study, we identified two functionally distinct HLADR⁺SIRP α ⁺CD14⁺CD64^{hi} MNPs that differentially accumulate in inflamed CD colon and further characterized their transcriptomic profile using scRNAseq. Firstly, the frequencies of CD163^{-dim} subpopulation, which was the major contributor of IL-1 β and IL-23 but not TNF- α , and more particularly the CD163⁻ cells significantly augmented in inflamed CD colon when compared to CD163^{hi} cells that did not accumulate and represented the predominant TNF- α -producing cell subset. The CD14⁺CD163⁻ subpopulation appeared to be part of the inflammatory landscape of CD since these cells did not infiltrate the paired non-inflamed CD colon or the colonic tissue of patients with infectious or drug-induced colitis. Notably, similar frequencies of HLADR⁺SIRP α ⁺CD14⁻ cells were detected in inflamed and non-inflamed colonic CD mucosa, unlike previous report of increased numbers of SIRP α ⁺CD11b⁺CD14⁻ bona fide cDC2s in the mucosa of patients with hyperemic epithelium.¹² Secondly, highly purified CD163⁻(P3) cells that morphologically resemble “monocyte-like cells”, but not CD163^{hi} (P4) cells resembling M ϕ , promoted memory Th17 into Th17/Th1 responses in an IL-1 β -dependent manner. Thirdly, scRNAseq revealed that P3 and P4 cells displayed a molecularly distinct signature. Finally, since our present findings further indicated that the percentage of CD163⁻ cells significantly correlated with SES-CD in an independent cohort of patients, we propose that mucosal P3 cells are associated with pathogenicity in CD.

The P3 cells appeared functionally distinct from the previously described CD14⁺CD163^{low} cells.³² As such, healthy, non-inflamed and inflamed CD colon comprise equal proportion of HLADR^{bright}CD14⁺CD163^{low} and CD163^{high} cells while HLADR^{dim}CD14⁺CD163^{low} cells were detected but not quantified in inflamed mucosa relative to healthy mucosa.³² In apparent contradiction with that study and our present findings, immunohistochemical analysis indicates that CD163-expressing cells accumulate in areas of active inflammation in IBD colon.⁴⁹ Furthermore, Ogino et al. provide evidence that only the HLADR^{bright}CD163^{low} or CD163^{hi} but not the HLADR^{dim}CD163^{low} cells polarize allogeneic naive peripheral blood CD4⁺ T cells and induce their differentiation into IL-17- or IFN- γ -producing T cells in a IL-1 β , IL-6, IL-23, and TGF β -dependent manner,³² corroborating earlier observations using unfractionated CD14⁺ MNPs.³⁷ The role of IL-1 β , IL-6, and TGF β in human Th17 cell polarization is well

established, whereas IL-23 only promotes Th17 cell expansion.⁵⁰ Noteworthy, the frequencies of naive CD4⁺ T cells are extremely low in intestinal mucosa⁵¹ and these two studies did not investigate the propensities of CD14⁺ MNPs to regulate colonic memory Th17 and Th17/Th1 responses, and thus to drive intestinal inflammation.

Here, we report that highly purified P3 cells, which are the predominant IL-1 β and IL-23-producing CD14⁺ subset in the inflamed colon, augmented mucosal effector Th17/Th1 cell responses with pathogenic potential. This effect was mediated by IL-1 β without excluding the implication of IL-23. Several lines of evidence argue for a key role of IL-1 β and IL-23 in driving CD. First, IL-1 β levels correlate with disease activity in CD patients⁵² and increases prior to disease relapse.⁵³ Second, IL-1 β upregulates IL-23 receptor on pathogenic T cells,⁴⁴ and vice versa, IL-23 augments IL-1 β receptor on T cells.⁵⁴ Third, IL-23 promotes gut inflammation in experimental colitis.⁴³ Finally, IL-1 β favors the accumulation and survival of colonic IL-17-secreting cells in a T-cell-dependent model of colitis.⁵⁴ This pro-survival function of IL-1 β on intestinal effector T cells might represent one of the mechanisms that governed the increased frequency of IL-17⁺IFN- γ ⁻ T cells observed in our study. Nonetheless, P3 cells as well as IL-1 β also augmented IL-17 expression per cell. In fact, drugs aiming to impair the effects of IL-1 β , such as IL-1 receptor antagonist (Anakinra), have been used in very early onset IBD patients, including chronic granulomatous disease and patients with IL-10 receptor mutations.⁵⁵ Furthermore, some authors⁵⁶ proposed that blocking IL-1 β could be beneficial in patients carrying *ATG16L1* or *NOD2* mutations, two genes associated with increased risk of CD. However, IL-1 β blockade could trigger or worsen IBD.⁵⁷ Yet, ongoing clinical trials indicate that IL-23 blockade appears to be beneficial in patients with CD.⁵⁸

TNF- α , which is abundantly produced by local effector T cells, still represents the major target in the therapeutic management of patients with CD.¹ We show here that frequencies of TNF- α -producing CD64^{hi}CD163^{hi} cells were significantly higher when compared to CD64^{hi}CD163^{-dim} cells that expressed very low levels of TNF- α . Although ~30% of CD patients were refractory to TNF- α antagonists in our cohort, treatment with biologics only or in combination with immunosuppressive drugs did not deplete either CD64^{hi}CD163^{-dim} cells, CD64^{hi}CD163^{hi} cells or TNF- α , IL-1 β , and IL-23-producing-cells. Nonetheless, TNF- α , like IL-1 β and IL-23, may exert a dual role in the intestinal mucosa. While TNF- α has pro-inflammatory properties, notably via interactions between membranous TNF- α on the surface of CD14⁺MNPs and TNFR2 expressed on T cells that results in T-cell survival, low levels of TNF- α may directly contribute to the maintenance of the epithelial cell barrier integrity.⁵⁹ IL-1 β as well as IL-23 participate in maintaining the integrity of gut epithelial barrier at least through the role they play on IL-22 secretion by ILC3.³¹ However, the protective function of ILC3 and IL-22 is also controversial since ILC3 drive experimental colitis through IL-1 β and IL-23-producing gut resident macrophages and IL-22.^{60–62} Collectively, targeting the IL-1 β pathway could be considered in the therapeutic arsenal for the management of CD, though caution should be exercised as the protective role of IL-1 β in the intestine could limit the safety of using IL-1 β pathway antagonists.

We further present evidence that P3 but not P4 cells might be implicated in the shift of Th17 cells towards Th17/Th1 profile. Although it would be very valuable to increase the number of experiments that compare P3 and P4 as well as P3/b and P4/b functionalities, the frequencies of these rare M ϕ -like cells (P4 and P4/b), and thus their yield, are very low in inflamed mucosa, precluding their purification in sufficient numbers from fresh biopsies to perform co-cultures experiments. Furthermore, surgical samples from CD patients heavily treated (multiple therapeutic failure) results in low cell recovery. Nonetheless, P4 cells that morphologically and molecularly resemble M ϕ , did not

accumulate or correlate with SES-CD, and were superior to inflammatory monocyte-like P3 cells in their propensity to express TNF- α and IL-10 in inflamed CD mucosa. Thus, P4 cells most likely do not drive intestinal memory Th17 responses corroborating M ϕ function in tumor ascites.⁶³

IL-17 is secreted by intestinal Th17 cells as well as $\gamma\delta$ T cells, both of which participate in mucosal homeostasis.⁶⁴ In that regard, the administration of anti-IL-17 mAb exacerbates colitis in mice⁴³ and humans.⁶⁵ However, IL-17/IFN- γ -secreting CD4⁺ T cells have been described as the pathogenic Th cell subset in the gut of IBD patients.^{5,40} Th17/Th1 and Th1 cells appear to predominate over Th17 cells in inflamed colon of CD patients, suggesting the plasticity of Th17 cell lineage. P3 cells and IL-1 β not only increased the frequency of IL-17/IFN- γ -secreting cells in colonic CD4⁺ T cells, but also promoted their pathogenic signature as shown by increased GM-CSF, TNF- α , and IL-6 secretion in memory CD4⁺ T cells. In that regard, IL-6 is known to enhance pathogenic T cell survival and promote the development of colonic carcinoma,⁶⁶ which is one of the long-term devastating complications associated with IBD.

Remarkably, unsupervised scRNAseq analysis that capture the entire HLADR⁺SIRP α ⁺ MNP population succeeded in providing finer cellular classification, with unbiased defined single cells clusters being significantly enriched for cells that were isolated according to the pre-defined gating strategy that used presence or absence of CD64, CD14, and CD163 expression. This analysis indicates that P3 and P4 cells, the two extreme subpopulations in CD163 expression spectrum within CD14⁺CD64^{hi} cells that omit the CD163^{dim} (Px), are both transcriptionally and functionally distinct. Interesting biology can be inferred from the discriminating genes for each cell cluster identified by scRNAseq. For example, markers for cluster E (significantly enriched for P3 cells) include *TREM1*, which is a member of the "Triggering Receptors Expressed on Myeloid cells" family, and *FCAR* reported to be highly expressed by unfractionated CD14⁺ MNPs and recently suggested to contribute to IBD pathogenesis.^{67–69} *FPR1*, also expressed by cluster E cells, was shown as a player involved in colorectal cancer tumor cell invasion, being also expressed in colorectal epitheliums and tumor infiltrating MNPs.⁷⁰ A recent integrative genomic approach identifies macrophage gene expression as a common signature, which includes *FPR1* among key regulators in IBD.⁷¹ Cluster F (significantly enriched for P4 cells) classifiers included candidates previously reported to be associated with mature and/or regulatory tissue M ϕ (e.g., *CD209/DC-SIGN*, *MRC1/CD206*, *CD163*, *CD163L1*, and *STAB1*),^{72,73} members of the complement system (e.g. *C2*, *C1QA*, *C1QB*, and *C1QC*) that may play a role in cellular cross-talk and polarization of MNPs; *MERTK*, and *Nr1h3/LXR α* , which is expressed on M ϕ and involved with clearance of apoptotic cells^{45,74}, as well as *IDH1*, *FOLR2*, *DNASE2*, *SLCOB21*, *DAB2*, and *VSIG4*, expressed by tissue inflammatory M ϕ and in vitro generated (M-CSF) M ϕ .⁷⁵ Furthermore, a more thorough analysis of scRNAseq data of the three patients allowed identification of four additional clusters beside clusters E and F in HLADR⁺SIRP α ⁺ MNPs. Cluster A, B, C were characterized by pDCs (cluster A) and conventional DCs (cluster B and C). Gene expression downregulation of several members of the UPS distinctively observed in cluster D cells may highlight the presence of non-reactive anergic macrophage phenotype, which has previously been reported in IBD.⁷⁶ Noteworthy, cross-presenting DCs (cDC1) were not identified as a separate cluster since these cells are HLADR⁺SIRP α ⁻ MNPs and obviously excluded from the captured population that was analyzed.

Importantly, the gating strategy used to initially isolate the P3 and P4 populations for functional studies excluded P1 intermediate as well as Px transitioning cells, which did not accumulate in the inflamed CD colon. P3 and P4 cell subsets are closely related and, analogous to monocyte-derived cells in mice and humans,^{13,16} could represent two distinct functional phenotypes

of a single population displaying a high degree of plasticity, with pro-inflammatory P3 converting towards Px transitioning cells, and then finally towards more anti-inflammatory P4 M ϕ -like cells. In the context of IBD, inflammation might slow down this maturation process, resulting in the accumulation of pro-inflammatory P3 cells in lesional sites. This hypothesis is currently being investigated, and out of the scope of the present study. Therefore, isolation of cells from each extreme of the spectrum defined by CD163 antigen intensity contributed to studying more "pure" sorted population and ultimately highlighted distinct roles of P3 and P4 cells. Remarkably, this molecular analysis identified novel classifiers beyond CD163 that enabled prospective isolation of TREM1⁺MERTK⁻CD209⁻ (P3/b), displaying similar functional characteristics to P3 cells.

Based on their phenotype and morphology, the P3 cells (TREM1⁺CD89⁺CD163⁻CD209⁻CD206⁻MERTK⁻) resemble M ϕ 1 (CD14⁺CD64⁺CD163^{dim}CD206⁻CD209^{dim}MERTK^{dim}), while P4 cells are comparable to M ϕ 4 (CD14⁺CD64⁺CD163^{high}CD206⁺CD209^{high}MERTK^{high}) subset, which are detected in healthy jejunum of patients with pancreatic cancer,¹³ or to HLADR^{high}CD14⁺CD163^{high}CD209^{high} cells in non-inflamed ileum of CD patients.¹⁶ However, neither M ϕ 1 nor M ϕ 4 in healthy human mucosa display the transcriptomic signature of P3 or P4 cells found here in inflamed CD colon.¹³ Interestingly, the human monocyte-like P3 and M ϕ -like P4 cells characterized in the present study shared common genes with murine colonic P1 (*TREM1*) and P4 (*MERTK*, *C1QA*, *C1QB*, and *C1QC*) CD11b⁺CD64⁺ cells, respectively.⁷⁷

Taken together, the functional snapshot analysis of HLADR⁺SIRP α ⁺ subpopulations in the colonic mucosa over a large cohort of CD patients yielded consistent results, regardless of the genetic background, age, gender, and disease states of our cohort, which included patients who were refractory to conventional anti-TNF- α or anti-IL-12p40 therapy. This highlights the broader biological relevance of our observations and the potential contribution of one particular mucosal HLADR⁺SIRP α ⁺CD14⁺CD64^{hi} subpopulation (i.e., the TREM1⁺CD209⁻MERTK⁻CD163⁻ (P3) cells), also identified by its molecular signature, to gut inflammation. Furthermore, we reproducibly showed the effect of P3 cells in promoting intestinal pathogenic Th17 cell profile. Based on our findings, we propose that impairing the accumulation and/or function of pathogenic CD14⁺CD64^{hi}CD163⁻ cells might attenuate ongoing colonic inflammation that have escaped TNF- α and/or IL-23 control, and thus might open avenues for novel therapeutic approaches in CD.

MATERIALS AND METHODS

Human clinical samples

All participants ($n = 186$) signed informed consent forms that have been approved by the Institutional Ethics Research Committee of the Centre Hospitalier de l'Université de Montréal and the Broad Institute of MIT and Harvard. Non-inflamed and inflamed colonic tissues (from the same patient) and MLNs were obtained from endoscopic biopsies or surgical resections. Five biopsies from non-inflamed and five biopsies from inflamed regions of the same patient were collected for staining, except for figure 1e ($n = 2$ biopsies); 10 biopsies were collected from inflamed region for co-culture experiments and scRNA-sequencing. Clinical information of all patients included in Figs. 1 to 9 and supplementary figures are shown in Table S4.

Cell isolation and flow cytometry

The colonic mucosa was first processed by enzymatic digestion with DNase I (Roche) and Collagenase D (Roche) followed by mechanical digestion with gentle MACS (Miltenyi Biotec) to isolate lamina propria mononuclear cells (LPMC). MLNs were digested mechanically to obtain cellular suspensions.¹¹

Ex vivo isolated LPMC cell suspension were immediately stained for surface markers, then fixed, permeabilized, and stained for intracytoplasmic cytokine expression using mAb listed in Table S5. FACS Aria II cell sorter was used for sorting MNP and T-cell populations in inflamed CD colon or MLNs. For single cell RNA-sequencing (scRNAseq) analysis, single cells were sorted into 96-well full-skirted Eppendorf plates chilled to 4 °C, pre-prepared with lysis buffer consisting of 10 µl of TCL buffer (Qiagen) supplemented with 1% β-mercaptoethanol. Single-cell lysates were sealed, vortexed, spun down at 300× g at 4 °C for 1 min, immediately placed on dry ice, and transferred for storage at −80 °C.

MNPs and CD4⁺ T cells co-cultures

CD4⁺ T cells (20 to 30 × 10³) or CCR6⁺CXCR3[−]CD62L^{low}CD4⁺ effector memory T cells (T_{EM}) (50 × 10³) isolated from inflamed CD colon or MLNs were stimulated with anti-CD3 and anti-CD28 coated beads (Miltenyi Biotec) or soluble anti-CD3 (1 µg/ml; Biologend), respectively, with no expansion in IL-2, and cultured: (a) with or without IL-1β (10 ng/ml; Peprotech), IL-12 (10 ng/ml; Peprotech), or IL-23 (10 ng/ml; R&D systems) for six days; (b) with or without autologous MNP subsets isolated from inflamed colonic mucosa at a 10:1 ratio for six days, in the presence of PGN (10 µg/ml; Sigma-Aldrich) and IgG1 (10 µg/ml; Biologend). Anti-IL-1β receptor (10 µg/ml) or anti-IL-12p40 (10 µg/ml) mAbs was added to some co-cultures. For all cultures: (a) RPMI 1640 medium with 10% fetal calf serum (FCS), 1% Penicillin/Streptomycin was used; (b) for intracytoplasmic staining, cells were re-stimulated after six days, with phorbol 12-myristate 13-acetate (PMA) (5 ng/ml; Sigma-Aldrich) and ionomycin (500 ng/ml; Calbiochem-Behring) for 6 h in the presence of brefeldin A (1 µg/ml; Calbiochem-Behring) for the last 3 h, then stained with CD3, fixed then permeabilized for intracytoplasmic cytokine staining (IL-17, IFN-γ, IL-6, and TNF-α) using mAb listed in Table S5.

Multiplex ELISA

IL-17, IFN-γ, IL-6, TNF-α, GM-CSF quantities were measured by multiplex assay (Eve Technologies, Calgary, AB, Canada) in the culture supernatants.

Single-cell RNA-sequencing—raw data samples and processing

The 414 sequenced cells consisted of 115 P1, 79 P2, 77 P4, 78 P3, and 65 Px samples (as depicted in Fig. 6a) from three patients, with 56 cells from patient x, 128 cells from patient y, and 230 cells from patient z (Fig. 6c). The raw sequencing reads were demultiplexed with standard bcl2fastq2 Illumina software (version 2.17.1.14) and aligned to the UCSC hg19 transcriptome with bowtie (version 0.12.7).⁷⁸ RSEM (version 1.2.1) was used to quantify gene expression level in transcripts per million (TPM)⁷⁹ and these expression data were log-transformed (log₂(TPM + 1)) before further analysis.

Single-cell expression data analyses were performed with the Seurat R package (version 1.4.0.5) following the strategy described in Villani et al, 2017.²⁷ The data were visualized in two dimensions by running t-distributed stochastic neighbor embedding (t-SNE) on the cell loadings for the first nine principle components. Heatmaps were used to visualize scaled (z-score) gene expression level (log₂(TPM + 1)) of identified markers.

Statistical analysis

Except for scRNAseq data, statistical analysis was performed with GraphPad Prism version 6 (GraphPad Software, La Jolla, CA, USA). Wilcoxon signed rank test (represented by *) and Mann–Whitney test (represented by §) were used. Threshold for significance was adjusted when indicated to account for test multiplicity. Friedman test and Kruskal–Wallis test were employed followed by Dunn's test (represented by #). Repeated measure Anova was employed followed by Bonferroni test (represented by π). For all tests, 1 symbol means P < 0.05; 2 symbols mean P < 0.01; 3 symbols

mean P < 0.001. Bar graph data are shown as mean ± s.e.m. unless otherwise stated. Spearman test was used to assess correlation.

ACKNOWLEDGEMENTS

We thank H. Mehta for critical reading and comments. We thank the subjects for donating the samples used in our study; the physicians who provided the samples: E.-J. Bernard, M. Boivin, S. Bouchard, J. Coté-Daigneault, L. Daoust, E. Deslandres, J. Dorais, B. Faulques, R. Lahaie, R. Leduc, M. Lemoyne, B. Panzini, P. Poitras, S. Sidani, and D. Von Renteln from gastroenterology unit; E. Debroux, R. Lougnarath, R. Ratelle, C. Richard, F. Swchenter, and R. Wassef from digestive tract surgery unit; B. Nguyen, G. Soucy from pathology department, at CHUM, Montreal; and C. Deslandres from gastroenterology unit at CHU Sainte-Justine, Montreal. We also thank the hematology department and the nurse C. Bergeron for their help. Canadian Institutes of Health Research (MOP#130533 (M.S.) and Banting Postdoctoral Fellowship (A.-C.V.)), Fonds de Recherche en Santé du Québec (L.C., M.Bs.), National Human Genome Research Institute Centers of Excellence in Genomics Science grant P50 HG006193 (N.H.), and the National Human Genome Research grant T32 HG002295 (S.S.; PI: Park, Peter J).

AUTHORS CONTRIBUTIONS

Conceptualization: L.C., M.Bs., M.R., S.S., A.-C.V., N.H., and M.S. Methodology and investigation: L.C., M.Bs., M.R., S.S., and A.-C.V. Resources: M.B., K.O., A.W., A.T., E.W., and L.C. Writing: L.C., M.Bs., A.-C.V., and M.S. Supervision: N.H., A.-C.V., and M.S. Funding acquisition: N.H. and M.S.

DATA AVAILABILITY

The data discussed in this publication have been deposited in NCBI's Gene Expression Omnibus, and are accessible through GEO Series accession number GSE140123 (<https://www.ncbi.nlm.nih.gov/geo/query/acc.cgi?acc=GSE140123>).

ADDITIONAL INFORMATION

The online version of this article (<https://doi.org/10.1038/s41385-018-0126-0>) contains supplementary material, which is available to authorized users.

Competing interests: The authors declare no competing interests.

Publisher's note: Springer Nature remains neutral with regard to jurisdictional claims in published maps and institutional affiliations.

REFERENCES

- de Souza, H. S. & Focchi, C. Immunopathogenesis of IBD: current state of the art. *Nat. Rev. Gastroenterol. Hepatol.* **13**(1), 13–27 (2016).
- Maloy, K. J. & Powrie, F. Intestinal homeostasis and its breakdown in inflammatory bowel disease. *Nature* **474**(7351), 298–306 (2011).
- Valatas, V., Bamias, G. & Kolios, G. Experimental colitis models: insights into the pathogenesis of inflammatory bowel disease and translational issues. *Eur. J. Pharmacol.* **759**, 253–264 (2015).
- Mowat, A. M. & Agace, W. W. Regional specialization within the intestinal immune system. *Nat. Rev. Immunol.* **14**(10), 667–685 (2014).
- Globig, A. M. et al. Comprehensive intestinal T helper cell profiling reveals specific accumulation of IFN-γ+IL-17+coproducing CD4+ T cells in active inflammatory bowel disease. *Inflamm. Bowel Dis.* **20**(12), 2321–2329 (2014).
- Chapuy, L. et al. Basophils increase in Crohn disease and ulcerative colitis and favor mesenteric lymph node memory TH17/TH1 response. *J. Allergy Clin. Immunol.* **134**(4), 978–981 (2014). e1.
- Lampinen, M. et al. Different regulation of eosinophil activity in Crohn's disease compared with ulcerative colitis. *J. Leukoc. Biol.* **84**(6), 1392–1399 (2008).
- Kuhl, A. A., Erben, U., Kredel, L. I. & Siegmund, B. Diversity of intestinal macrophages in inflammatory bowel diseases. *Front. Immunol.* **6**, 613 (2015).
- Bernink, J. H. et al. Human type 1 innate lymphoid cells accumulate in inflamed mucosal tissues. *Nat. Immunol.* **14**(3), 221–229 (2013).
- Fuchs, A. et al. Intraepithelial type 1 innate lymphoid cells are a unique subset of IL-12- and IL-15-responsive IFN-γ-producing cells. *Immunity* **38**(4), 769–781 (2013).
- Baba, N. et al. CD47 fusion protein targets CD172a+ cells in Crohn's disease and dampens the production of IL-1β and TNF. *J. Exp. Med.* **210**(6), 1251–1263 (2013).
- Watchmaker, P. B. et al. Comparative transcriptional and functional profiling defines conserved programs of intestinal DC differentiation in humans and mice. *Nat. Immunol.* **15**(1), 98–108 (2014).

13. Bujko, A., Atlasy, N. & Landsverk, O. J. B. Transcriptional and functional profiling defines human small intestinal macrophage subsets. *J. Exp. Med.* **215**(2), 441–458 (2018).
14. Williams, M. & van de Laar, L. A Hitchhiker's guide to myeloid cell subsets: practical implementation of a novel mononuclear phagocyte classification system. *Front. Immunol.* **6**, 406 (2015).
15. Smith, P. D. et al. Intestinal macrophages and response to microbial encroachment. *Mucosal Immunol.* **4**(1), 31–42 (2011).
16. Bain, C. C. et al. Resident and pro-inflammatory macrophages in the colon represent alternative context-dependent fates of the same Ly6Chi monocyte precursors. *Mucosal Immunol.* **6**(3), 498–510 (2013).
17. Sakuraba, A. et al. Th1/Th17 immune response is induced by mesenteric lymph node dendritic cells in Crohn's disease. *Gastroenterology* **137**(5), 1736–1745 (2009).
18. Loschko, J. et al. Absence of MHC class II on cDCs results in microbial-dependent intestinal inflammation. *J. Exp. Med.* **213**, 517–534 (2016).
19. Fortin, G. et al. A role for CD47 in the development of experimental colitis mediated by SIRPalpha+CD103⁻ dendritic cells. *J. Exp. Med.* **206**(9), 1995–2011 (2009).
20. Bernardo, D. et al. Chemokine (C-C Motif) receptor 2 mediates dendritic cell recruitment to the human colon but is not responsible for differences observed in dendritic cell subsets, phenotype, and function between the proximal and distal colon. *Cell. Mol. Gastroenterol. Hepatol.* **2**(1), 22–39 (2016). e5.
21. Williams, M. et al. Unsupervised high-dimensional analysis aligns dendritic cells across tissues and species. *Immunity* **45**(3), 669–684 (2016).
22. Mann, E. R. et al. Compartment-specific immunity in the human gut: properties and functions of dendritic cells in the colon versus the ileum. *Gut* **65**(2), 256–270 (2016).
23. Sichien, D., Lambrecht B. N., Williams M. & Scott C. L. Development of conventional dendritic cells: from common bone marrow progenitors to multiple subsets in peripheral tissues. *Mucosal Immunol.* **10**, 831–844 (2017).
24. Cerovic, V. et al. Intestinal CD103(–) dendritic cells migrate in lymph and prime effector T cells. *Mucosal Immunol.* **6**(1), 104–113 (2013).
25. Diehl, G. E. et al. Microbiota restricts trafficking of bacteria to mesenteric lymph nodes by CX(3)CR1(hi) cells. *Nature* **494**(7435), 116–120 (2013).
26. Schroder, M. et al. CD1c-expression by monocytes—implications for the use of commercial CD1c+dendritic cell isolation kits. *PLoS ONE* **11**(6), e0157387 (2016).
27. Villani, A. C. & et al. Single-cell RNA-seq reveals new types of human blood dendritic cells, monocytes, and progenitors. *Science* **356**, 6335 (2017).
28. Ng, S. C. et al. Worldwide incidence and prevalence of inflammatory bowel disease in the 21st century: a systematic review of population-based studies. *Lancet* **390**(10114), 2769–2778 (2018).
29. Grimm, M. C. et al. Direct evidence of monocyte recruitment to inflammatory bowel disease mucosa. *J. Gastroenterol. Hepatol.* **10**(4), 387–395 (1995).
30. Kamada, N. et al. Unique CD14 intestinal macrophages contribute to the pathogenesis of Crohn disease via IL-23/IFN-gamma axis. *J. Clin. Invest.* **118**(6), 2269–2280 (2008).
31. Longman, R. S. et al. CX(3)CR1(+) mononuclear phagocytes support colitis-associated innate lymphoid cell production of IL-22. *J. Exp. Med.* **211**(8), 1571–1583 (2014).
32. Ogino, T. et al. Increased Th17-inducing activity of CD14+CD163 low myeloid cells in intestinal lamina propria of patients with Crohn's disease. *Gastroenterology* **145**(6), 1380–1391 (2013). e1.
33. Barman, S. et al. Identification of a human intestinal myeloid cell subset that regulates gut homeostasis. *Int. Immunol.* **28**(11), 533–545 (2016).
34. Thiesen, S. et al. CD14(hi)HLA-DR(dim) macrophages, with a resemblance to classical blood monocytes, dominate inflamed mucosa in Crohn's disease. *J. Leukoc. Biol.* **95**(3), 531–541 (2014).
35. Magnusson, M. K. et al. Macrophage and dendritic cell subsets in IBD: ALDH(+) cells are reduced in colon tissue of patients with ulcerative colitis regardless of inflammation. *Mucosal Immunol.* **9**(1), 171–182 (2016).
36. Sandborn, W. J. et al. Vedolizumab as induction and maintenance therapy for Crohn's disease. *N. Engl. J. Med.* **369**(8), 711–721 (2013).
37. Kamada, N. et al. Human CD14+ macrophages in intestinal lamina propria exhibit potent antigen-presenting ability. *J. Immunol.* **183**(3), 1724–1731 (2009).
38. Ahern, P. P. et al. Interleukin-23 drives intestinal inflammation through direct activity on T cells. *Immunity* **33**(2), 279–288 (2010).
39. Annunziato, F. et al. Phenotypic and functional features of human Th17 cells. *J. Exp. Med.* **204**(8), 1849–1861 (2007).
40. Ramesh, R. et al. Pro-inflammatory human Th17 cells selectively express P-glycoprotein and are refractory to glucocorticoids. *J. Exp. Med.* **211**(1), 89–104 (2014).
41. Cosmi, L., Liotta, F., Maggi, E., Romagnani, S. & Annunziato, F. Th17 and non-classic Th1 cells in chronic inflammatory disorders: two sides of the same coin. *Int. Arch. Allergy Immunol.* **164**(3), 171–177 (2014).
42. Sano, T. et al. An IL-23R/IL-22 circuit regulates epithelial serum amyloid A to promote local effector Th17 responses. *Cell* **163**(2), 381–393 (2015).
43. Maxwell, J. R. et al. Differential roles for interleukin-23 and interleukin-17 in intestinal immunoregulation. *Immunity* **43**(4), 739–750 (2015).
44. Kleinschek, M. A. et al. Circulating and gut-resident human Th17 cells express CD161 and promote intestinal inflammation. *J. Exp. Med.* **206**(3), 525–534 (2009).
45. Jakubzick, C. V., Randolph, G. J. & Henson, P. M. Monocyte differentiation and antigen-presenting functions. *Nat. Rev. Immunol.* **17**(6), 349–362 (2017).
46. Segura, E. & Amigorena, S. Inflammatory dendritic cells in mice and humans. *Trends Immunol.* **34**(9), 440–445 (2013).
47. Daperno, M. et al. Development and validation of a new, simplified endoscopic activity score for Crohn's disease: the SES-CD. *Gastrointest. Endosc.* **60**(4), 505–512 (2004).
48. Bernink, J. H. et al. Interleukin-12 and -23 Control Plasticity of CD127(+) Group 1 and Group 3 innate lymphoid cells in the intestinal lamina propria. *Immunity* **43**(1), 146–160 (2015).
49. Franze, E. et al. Lesional accumulation of CD163⁺ expressing cells in the gut of patients with inflammatory bowel disease. *PLoS ONE* **8**(7), e69839 (2013).
50. Stadhouders, R., Lubberts, E. & Hendriks, R. W. A cellular and molecular view of T helper 17 cell plasticity in autoimmunity. *J. Autoimmun.* **87**, 1–15 (2018).
51. Granot, T. et al. Dendritic cells display subset and tissue-specific maturation dynamics over human life. *Immunity* **46**(3), 504–515 (2017).
52. Casini-Raggi, V. et al. Mucosal imbalance of IL-1 and IL-1 receptor antagonist in inflammatory bowel disease. A novel mechanism of chronic intestinal inflammation. *J. Immunol.* **154**(5), 2434–2440 (1995).
53. Schreiber, S. et al. Tumour necrosis factor alpha and interleukin 1beta in relapse of Crohn's disease. *Lancet* **353**(9151), 459–461 (1999).
54. Coccia, M. et al. IL-1beta mediates chronic intestinal inflammation by promoting the accumulation of IL-17A secreting innate lymphoid cells and CD4(+) Th17 cells. *J. Exp. Med.* **209**(9), 1595–1609 (2012).
55. Shouval, D. S. et al. Interleukin 1beta mediates intestinal inflammation in mice and patients with interleukin 10 receptor deficiency. *Gastroenterology* **151**(6), 1100–1104 (2016).
56. Otipari, A. & Franchi, L. Role of inflammasomes in intestinal inflammation and Crohn's disease. *Inflamm. Bowel Dis.* **21**(1), 173–181 (2015).
57. Huggle, B., Speth, F. & Haas, J. P. Inflammatory bowel disease following anti-interleukin-1-treatment in systemic juvenile idiopathic arthritis. *Pediatr. Rheumatol. Online J.* **15**(1), 16 (2017).
58. Sands, B. E. et al. Efficacy and safety of MEDI2070, an antibody against interleukin 23, in patients with moderate to severe Crohn's disease: a phase 2a study. *Gastroenterology* **153**(1), 77–86 (2017). e6.
59. Billmeier, U., Dieterich, W., Neurath, M. F. & Atreya, R. Molecular mechanism of action of anti-tumor necrosis factor antibodies in inflammatory bowel diseases. *World J. Gastroenterol.* **22**(42), 9300–9313 (2016).
60. Buonocore, S. et al. Innate lymphoid cells drive interleukin-23-dependent innate intestinal pathology. *Nature* **464**(7293), 1371–1375 (2010).
61. Eken, A., Singh, A. K., Treuting, P. M. & Oukka, M. IL-23R+innate lymphoid cells induce colitis via interleukin-22-dependent mechanism. *Mucosal Immunol.* **7**(1), 143–154 (2014).
62. Bauche, D. et al. LAG3(+) regulatory T cells restrain interleukin-23-producing CX3CR1(+) gut-resident macrophages during group 3 innate lymphoid cell-driven colitis. *Immunity* **49**(2), 342–352 (2018). e5.
63. Segura, E. et al. Human inflammatory dendritic cells induce Th17 cell differentiation. *Immunity* **38**(2), 336–348 (2013).
64. Stockinger, B. & Omenetti, S. The dichotomous nature of T helper 17 cells. *Nat. Rev. Immunol.* **17**(9), 535–544 (2017).
65. Hueber, W. et al. Secukinumab, a human anti-IL-17A monoclonal antibody, for moderate to severe Crohn's disease: unexpected results of a randomised, double-blind placebo-controlled trial. *Gut* **61**(12), 1693–1700 (2012).
66. Punkenburg, E. et al. Batf-dependent Th17 cells critically regulate IL-23 driven colitis-associated colon cancer. *Gut* **65**, 1139–1150 (2016).
67. Schenk, M., Bouchon, A., Seibold, F. & Mueller, C. TREM-1—expressing intestinal macrophages crucially amplify chronic inflammation in experimental colitis and inflammatory bowel diseases. *J. Clin. Invest.* **117**(10), 3097–3106 (2007).
68. Kokten, T. et al. TREM-1 inhibition restores impaired autophagy activity and reduces colitis in mice. *J. Crohns Colitis* **12**, 230–244 (2018).
69. Brynjolfsson, S. F. et al. An antibody against triggering receptor expressed on myeloid cells 1 (TREM-1) dampens proinflammatory cytokine secretion by lamina propria cells from patients with IBD. *Inflamm. Bowel Dis.* **22**(8), 1803–1811 (2016).
70. Li, S. Q. et al. The expression of formyl peptide receptor 1 is correlated with tumor invasion of human colorectal cancer. *Sci. Rep.* **7**(1), 5918 (2017).

71. Peters, L. A. et al. A functional genomics predictive network model identifies regulators of inflammatory bowel disease. *Nat. Genet.* **49**(10), 1437–1449 (2017).
72. Gonzalez-Dominguez, E. et al. CD163L1 and CLEC5A discriminate subsets of human resident and inflammatory macrophages in vivo. *J. Leukoc. Biol.* **98**(4), 453–466 (2015).
73. Murray, P. J. et al. Macrophage activation and polarization: nomenclature and experimental guidelines. *Immunity* **41**(1), 14–20 (2014).
74. A-Gonzalez, N. et al. Phagocytosis imprints heterogeneity in tissue-resident macrophages. *J. Exp. Med.* **214**(5), 1281–1296 (2017).
75. Goudot, C. et al. Aryl hydrocarbon receptor controls monocyte differentiation into dendritic cells versus macrophages. *Immunity* **47**(3), 582–596 (2017). e6.
76. Hetzenecker, A. M. et al. Downregulation of the ubiquitin-proteasome system in normal colonic macrophages and reinduction in inflammatory bowel disease. *Digestion* **86**(1), 34–47 (2012).
77. Schridde, A. et al. Tissue-specific differentiation of colonic macrophages requires TGFbeta receptor-mediated signaling. *Mucosal Immunol.* **10**(6), 1387–1399 (2017).
78. Langmead, B., Trapnell, C., Pop, M. & Salzberg, S. L. Ultrafast and memory-efficient alignment of short DNA sequences to the human genome. *Genome Biol.* **10**(3), R25 (2009).
79. Li, B. & Dewey, C. N. RSEM: accurate transcript quantification from RNA-Seq data with or without a reference genome. *BMC Bioinforma.* **12**, 323 (2011).

